Potential Vorticity Diagnostics of Hurricane Movement. Part I: A Case Study of Hurricane Bob (1991)

CHUN-CHIEH WU*

Program in Atmospheric Sciences, Princeton University, Princeton, New Jersey

KERRY A. EMANUEL

Center for Meteorology and Physical Oceanography, Massachusetts Institute of Technology, Cambridge, Massachusetts

(Manuscript received 30 November 1993, in final form 6 May 1994)

ABSTRACT

Potential vorticity (PV) diagnostics are applied to evaluate the control by the large-scale environment of hurricane movement and, more importantly, to assess the storm's influence on its own track. As a first application of these diagnostics, an observational case study of Hurricane Bob (1991) is presented using the twice-daily National Meteorological Center Northern Hemisphere final analyses gridded datasets. Defining the seasonal climatology as the mean reference state, piecewise potential vorticity inversions are performed under the nonlinear balance condition. This allows one to determine the balanced flows associated with any individual perturbation of PV. By examining the balanced flows at the central position of the hurricane, one can identify the influence of each PV perturbation on hurricane movement. The *hurricane advection flow* is also defined as the balanced flow at the storm center associated with the whole PV distribution, excluding the positive PV anomaly of the hurricane itself.

The results from the observational study of Bob show that the hurricane advection flow is a good approximation to the real storm motion. The results also show that the balanced flows associated with the climatological mean PV and perturbation PV distribution in both the lower and upper troposphere are both important in contributing to Bob's movement. However, it is difficult to separate PV anomalies directly or indirectly attributable to the storm from ambient PV anomalies. Results from other cases will be presented in a companion paper.

1. Introduction

Most previous studies of tropical cyclone motion have considered steering by the mean flow (e.g., Chan and Gray 1982) and the effect of uniform background potential vorticity gradients, that is, the evolution of barotropic vortices in a barotropic flow (e.g., Fiorino and Elsberry 1989). However, Wu and Emanuel [1993 (hereafter WEM), 1994], Shapiro (1992), and Flatau et al. (1994) have shown that the propagation of a baroclinic hurricane, embedded in a nonuniform background potential vorticity gradient, could be different from the traditional expectation, based on the so-called β effect (e.g., Chan and Williams 1987). WEM designed an idealized numerical model to explore the effect of background vertical shear on tropical cyclone motion. Based on the theory of slantwise moist convection and output from detailed numerical simulations (Rotunno and Emanuel 1987), WEM suggested that hurricanes may be considered as local sources of nearly zero potential vorticity (PV) air in the upper troposphere. Specifically, they showed that in the absence of background PV gradients, Northern (Southern) Hemisphere tropical cyclones should drift relative to the mean flow in a direction to the left (right) of the background vertical shear because of the flow associated with the upper negative PV anomaly, which is displaced downshear from the center of the surface cyclone.

In this work, we apply potential vorticity (PV) diagnostics in an attempt to understand hurricane steering. We undertake three case studies involving Hurricane Bob (1991), Tropical Storm Ana (1991), and Hurricane Andrew (1992). Piecewise potential vorticity inversions are performed under nonlinear balance conditions. This allows one to determine the balanced flow associated with individual PV perturbations. By examining the balanced flow near the central position of a hurricane, one can quantitatively study how each PV anomaly contributes to hurricane motion and how

* Current affiliation: Department of Atmospheric Sciences, National Taiwan University, Taipei, Taiwan.

Corresponding author address: Dr. Chun-Chieh Wu, Dept. of Atmospheric Sciences, National Taiwan University, 61, Ln 144, Sec 4, Keelung Rd., 10772 Taipei, Taiwan.

well storm-generated PV anomalies affect storm motion. The main objectives of this study are as follows:

1) to understand how a hurricane may influence its evolution by creating PV anomalies in the environment (such as the through the β effect and by generating upper-level negative PV anomalies) that in turn affect hurricane motion,
2) to provide a better definition of hurricane advection (steering) flow, and
3) to quantitatively understand how individual synoptic or larger-scale weather systems influence hurricane motion.

This work is divided into two consecutive papers. This first paper provides a review of the subject and specifies the questions we wish to address. A case study of Bob is also presented. The second paper (Wu and Emanuel 1995) presents the results from two other case studies (Tropical Storm Ana of 1991 and Hurricane Andrew of 1992) and summarizes this work.

This paper is organized as follows. In section 2, the literature and background related to this work are reviewed. The methodology of this study is discussed in section 3. The results from the case study of Bob are presented in section 4. Finally, section 5 summarizes this paper.

2. Background

a. Hurricane movement

The steering concept is based on the assumption that tropical cyclones are isolated vorticity anomalies embedded in a background environment of larger-scale flow and thus move with a so-called "steering" flow, generally taken to be a pressure-weighted vertical average of the horizontal flow in the troposphere surrounding the hurricane (e.g., Chan and Gray 1982). The pressure level at which the speed and direction of the surrounding winds best correlate with the track of the storms is generally referred to as the steering level. It has been shown (Neumann 1979) that such a steering flow can account for about 80% of the variability in 24-h tropical cyclone motion in the Atlantic.

Because the cyclone itself is part of the large-scale flow, which varies with altitude, defining an appropriate steering current is difficult. In fact, there is no unique way to determine the steering flow. Uncertainty in the hurricane-steering relationship may arise not only from the inaccuracies inherent in determining the initial fields over the data-sparse oceanic regions but also from the ambiguous definition of the steering flow. It is not clear which level represents the best steering level, what is the best definition of the annular average (the azimuthal average flow surrounding hurricanes), and how definitions of steering flow should differ among tropical cyclones having differing characteristics, including storm intensity, size, location, track directions, and track displacements. Even so, many studies have shown that the basic current in the middle tropospheric or a deeper layer mean flow may represent the hurricane steering flow (Jordan 1952; Miller 1958; Miller and Moore 1960; George and Gray 1976; Neumann 1979; Brand et al. 1981; Chan and Gray 1982; Chan 1985; Dong and Neumann 1986).

Jordan was one of the pioneers in employing real data to test the steering concept. He showed that, on average, tropical storms move in the direction and with the speed of a steering current defined as the pressure-weighted mean flow from the surface to 300 mb, extending over an 8° latitude band centered on the storm. Miller and Moore used a grid system to compute the geostrophic components around tropical cyclones at the 700-, 500-, and 300-mb levels. They found that the 700- and 500-mb flows appear to be equally good in predicting the subsequent 24-h hurricane motion. George and Gray composited 10 years of rawinsonde data from 30 stations in the western North Pacific. They showed that tropical cyclone motion is well correlated with the surrounding lower troposphere flow fields averaged over a 1°–7° radial band. They also found that this general correlation of flow features applies equally well for different types of storms.

There do appear to be systematic deflection of hurricane motion from steering flows defined in this way, however, and there are inconsistencies in the assessment of such deflections. For example, Miller (1958) found that most tropical storms move to the right of the steering flows, whereas George and Gray's results show that for western North Pacific storms there is a leftward deviation from the middle-tropospheric mean flow. Also, Brand et al. found that most western North Pacific storms move to the left of the 500-mb flow at middle and higher latitudes but to the right at lower latitudes. Dong and Neumann suggested that these contradictions may be due to an improper stratification of cases.

A thorough composite observational study by Chan and Gray also supports the steering concept, though a systematic directional deviation between what they define as the steering flow and storm motion was generally found. Chan and Gray show that the middle-tropospheric (500–700 mb) 5°–7° latitude-radius annular average wind has the best correlation with the cyclone motion. They found that tropical cyclones in the Northern Hemisphere move about 10°–20° to the left of this steering flow and those in the Southern Hemisphere move about 10° to the right. They also found that tropical cyclones, in general, move about 1 m s^{-1} faster than the steering flow. Smith et al. (1990) and Ulrich and Smith (1991) have used a barotropic model simulation to assess the applicability of the annular average flow in defining an appropriate environmental current. They found that the vortex motion generally agrees very well with the flow calculated in the inner circular domain (e.g., of radius 1° latitude) but is less

accurate when using an outer average (e.g., 3°–5° or 5°–7°).

Dong and Neumann demonstrated that there is considerable uncertainty about which layer or level determines the steering flow. They suggested that a minimum forecast error would be realized by using the middle-tropospheric levels or a deep-layer average in statistical prediction schemes, while the height of the best steering level or the depth of the best deep-layer steering increases in proportion to hurricane intensity. Similar results were found by Velden and Leslie (1991) in their study of cyclones in the Australian region.

An individual case study of Hurricane Josephine (1984) was conducted by Franklin (1990). He employed wind information measured from Omega dropwindsondes during the "synoptic flow" experiments by the Hurricane Research Center. He showed that Hurricane Josephine generally moved in the direction of the 700-mb flow and with the speed of approximately the 500-mb flow. However, he pointed out that the 5°–7° band average wind indicates a large vertical wind shear, and he demonstrated that in an environment with a mean vertical shear, the predicted movement of the storm was very sensitive to assumptions about the altitude at which the steering flow is defined.

By using the NMC T80 global analysis and the output from the Geophysical Fluid Dynamics Laboratory hurricane model, Kurihara et al. (1990) has shown that the vertically integrated large-scale flow field, with the disturbance (hurricane vortex) field removed by the application of a spatial smoothing operator, is a good approximation to the actual hurricane track. Recent observational studies (Roux and Marks 1991; Marks et al. 1992) have employed airborne Doppler radar data to construct the three-dimensional wind field near the inner core of Hurricanes Hugo (1989) and Norbert (1984). They found that the motion of each storm is close to the flow averaged over some small domain near the center and that the vortex motion generally agrees very well with the flow calculated in the inner circular domain (e.g., of radius 1° latitude). These findings reflect the original concept of steering flow, which regards the hurricane as a point vortex that it is advected by the mean environmental flow at its center. It should be mentioned that the reason why many studies have used an annular average to represent the hurricane steering flow is because of the paucity of meteorological observations in and around hurricanes. The band average is purely an empirical attempt to approximate the hurricane advection flow.

At any instant in time, hurricane motion is dominated by the vertically averaged instantaneous flow through its center. [As indicated by Roux and Marks (1991), each storm's motion is close to its depth-averaged wind velocity in the inner core region.] The relative motion of the hurricane with respect to the steering flow depends exactly upon how the latter is defined. As indicated in Smith and Ulrich (1993), it is possible that an inappropriate representation of the steering flow or the environmental flow across vortex center could result in a spurious inference of hurricane movement. The "propagation" effects detected from observational studies (e.g., Carr and Elsberry 1990; Franklin 1990) are with respect to a fairly large-scale average flow, not the instantaneous flow through the storm center. The differences among some barotropic models (e.g., Chan and Williams 1987; Fiorino and Elsberry 1989) may be interpreted as the differences in the way these models perturb the environmental (potential) vorticity fields in such a way as to change the mean flow through the storm center. For example, the "β effect" describes a process in which a hurricane vortex embedded in a background planetary vorticity gradient induces dipole vorticity gyres that change the steering (advection) of the vortex. The word "propagation" only has meaning with respect to large-scale average flows.

b. Potential vorticity diagnostics

The diagnostic use of potential vorticity has been reviewed by Hoskins et al. (1985). Ertel's potential vorticity is defined as

$$Q = \frac{\boldsymbol{\xi}}{\rho} \cdot \nabla\theta,$$

where Q represents PV, ρ is the density, $\boldsymbol{\xi}$ is the absolute vorticity vector, and θ is the potential temperature. There are three significant properties of PV that make it a particularly useful diagnostic quantity:

1) the conservation principle, which states that PV is conserved following adiabatic and frictionless motion;
2) the invertibility principle, which states that given a distribution of PV, a prescribed balance condition, and boundary conditions, balanced mass and wind fields can be recovered; and
3) the superposition principle, which states that when two PV anomalies of the same (opposite) sign are brought closer to each other, the mass-integrated total perturbation energy will increase (decrease).

From the invertibility relation, all of the dynamic information can be recovered from a single field, PV, given an appropriate balance condition. Consequently, the dynamics in a fluid system is succinctly contained in the PV field evolution. Since the atmosphere is generally observed to contain various features with signatures in the PV field, the quasi-conservation property of PV allows one to easily identify the movement and change in shape and structure of these features.

Davis and Emanuel (1991) applied potential vorticity diagnostics to the analysis of extratropical cyclogenesis. They inverted PV using a nonlinear balance condition. Moreover, they derived a method for per-

forming a piecewise PV inversion under a nonlinear balance condition. One important feature of their piecewise inversion scheme is that the geopotential perturbations associated with each PV anomaly are linearly superposable. In other words, the summation of the balanced geopotential fields associated with each individual PV perturbation is the total geopotential balanced field. In this way, they were able to demonstrate how specific parts of the PV anomaly distribution interact with one another, in an attempt to gain a clearer and more coherent picture of the development of cyclones. Their methodology has been adopted in this study.

Potential vorticity methods have proven useful in understanding synoptic- and large-scale midlatitude dynamics and are becoming more widely applied to tropical motion systems. Molinari (1993) showed that the intensity change of Hurricane Helen (1980) can be related to the evolution of an upper-tropospheric PV anomaly. Reilly (1992) conducted an observational case study and found that supertropospheric PV advection plays an important role in tropical cyclogenesis. Montgomery and Farrell (1993) also investigated the influence of upper-level potential vorticity disturbances on tropical cyclone formation within the context of two simple nonlinear balance models that incorporate moist processes. Their results agree with the indication from observations that the early stages of tropical cyclogenesis are essentially a slow manifold phenomenon and thus can be regarded as a balanced response to slowly interacting upper- and lower-level PV fields.

Our approach presumes that hurricane motion is also closely connected to the interaction of the hurricane with its environmental PV fields and may be better understood in the context of quasi-balanced dynamics.

c. *Potential vorticity view of the hurricane advection flow*

Smith and Ulrich (1993) have shown that hurricane motion in a barotropic background flow can be regarded as a barotropic process, in which the vortex is simply advected by the environmental flow across the vortex core. Within a three-dimensional perspective, the hurricane appears as a strong and localized positive PV anomaly in the lower and middle troposphere. Since this PV patch is so localized, it may be approximated as a "point vortex" in the sense that the flow due to all other PV anomalies varies little over the scale of the vortex patch. From this point of view, the movement of a hurricane should be dominated by some vertical integral of the instantaneous flow through its center. This argument has been made in the aforementioned observational studies (Roux and Marks 1991; Marks et al. 1992). To distinguish the instantaneous local flow through the hurricane center from large-scale average flows, we shall refer to the local, instantaneous flow through the hurricane center as the *hurricane advection flow.*

In reality, it is difficult to accurately derive the advection flow in the center of a hurricane partly because of the insufficient observations in the storm region, because the advection flow may vary with altitude, and because the component of the wind through the storm center can be masked by the strong azimuthal winds surrounding the hurricane. For example, there can be large uncertainty in estimating the advection flow when the observational data cannot accurately locate the hurricane center. To avoid these problems, researchers have tended to construct an annular and tropospheric mean flow to average out the azimuthal winds and thus find the steering flow, and it has been shown by Chan and Gray (1982) that the middle-tropospheric (500–700 mb) 5°–7° latitude-radius average wind has the best correlation with the cyclone motion. Though there is generally good agreement between this mean flow and hurricane motion, this estimate of steering flow is susceptible to large errors arising from the paucity of data.

Though hurricanes are distinct isolated vortices, they are embedded within background flows that have a rich and variable structure. The environment has a significant influence on the vortex motion. For example, as a hurricane moves, it interacts with large-scale circulations and adjacent synoptic-scale systems (typical examples are the subtropical high over the ocean and midlatitude upper-tropospheric waves). Thus, the orientation and strength of the hurricane steering current changes in response to the normal propagation and development of large-scale pressure ridges and troughs in the atmosphere. It is important to understand how individual synoptic or large-scale features interact with the storm track. Since the nonlinear balance condition is a good approximation for synoptic and large-scale flows in the Tropics (Haltiner and Williams 1980), the PV approach provides a convenient basis for diagnosing how synoptic and large-scale dynamical systems interact with hurricanes. By performing piecewise potential vorticity inversions under nonlinear balance conditions, we can determine the balanced flow associated with individual PV perturbations, including those induced by the storm itself. Then, by examining the components of the balanced flow at the hurricane center, we can identify how each PV anomaly influences hurricane movement.

3. Methodology

a. *Data*

The data used are taken from the final global analyses of the National Meteorological Center (NMC) archived on a 2.5 × 2.5 latitude–longitude grid. Geopotential height, temperature, and horizontal winds are available at 0000 and 1200 UTC on 10 mandatory isobaric surfaces. The tracks and intensities of the hurricanes in this study are taken from the National Hurri-

cane Center (NHC) postseason analyses for both the 1991 and 1992 seasons (1991 and 1992 Hurricane Preliminary Reports). The domain we use extends from 2.5° to 62.5°N and from 120° to 30°W. The GEMPAK package is used for analysis and for plotting.

The primary data source of NMC analyses (Dey 1989) is the conventional surface and upper-air network (including radiosondes), with supplementary data supplied by pilot balloons, cloud-track winds, aircraft reports, and remotely sensed temperature soundings. Using a spectral statistical interpolation technique (optimal interpolation before 1991), raw observations are used to correct the first-guess fields provided by a 6-h forecast from the NMC global spectral model (Kanamitsu 1989; Kanamitsu et al. 1991) initialized using the previous analysis. Therefore, although NMC analyses cannot resolve all the small-scale features, such as the detailed structure of hurricanes, they presumably can represent with some accuracy synoptic- and large-scale features that can be resolved by information in the database and should also be able to retain these features for some time even after adequate resolution by observations has been lost. Although there are uncertainties in the NMC analysis of divergence over the tropical region (Trenberth and Olson 1988), our study primarily focuses on the balanced part of the flow field.

It should be kept in mind that smaller-scale disturbances originating over data-sparse areas may not be captured by the NMC analyses. For example, an upper-level PV anomaly diabatically generated by a hurricane may not be well represented. Also, the hurricane itself is too small in scale to be represented adequately, and its location may be in error.

b. *Potential vorticity diagnostics*

1) TOTAL PV INVERSION

Davis and Emanuel's (1991, hereafter DE) method for PV inversion is employed in this study. The balance equation, originally derived by Charney (1955), is, in spherical coordinates,

$$\nabla^2\Phi = \nabla\cdot(f\nabla\Psi) + \frac{2}{a^4\cos^2\phi}\frac{\partial(\Psi_\lambda, \Psi_\phi)}{\partial(\lambda, \phi)}, \quad (3.1)$$

where Φ is the geopotential, Ψ is the streamfunction of the nondivergent flow, f is the Coriolis parameter, λ is longitude, ϕ is latitude, a is the radius of the earth, and the last operator on the right-hand side of (3.1) is the Jacobian. The approximate definition of Ertel's PV in π coordinates is

$$q = -\frac{g\kappa\pi}{p}\left(\eta\frac{\partial\theta}{\partial\pi} - \frac{1}{a\cos\phi}\frac{\partial v}{\partial\pi}\frac{\partial\theta}{\partial\lambda} + \frac{1}{a}\frac{\partial u}{\partial\pi}\frac{\partial\theta}{\partial\phi}\right), \quad (3.2)$$

where $\kappa = R_d/C_p$, p is the pressure, η is the vertical component of absolute vorticity, θ is the potential temperature, and π is the Exner function:

$$\pi = C_p\left(\frac{p}{p_0}\right)^\kappa.$$

We use the hydrostatic approximation,

$$\theta = -\frac{\partial\Phi}{\partial\pi}.$$

Also, replacing the total wind by the nondivergent wind

$$\mathbf{V} = \mathbf{k}\times\nabla\Psi,$$

we can solve the system of two equations (3.1) and (3.2) for the two unknowns Φ and Ψ, given the distribution of q, θ on the upper and lower boundaries, and Φ and Ψ on the lateral boundaries. We use the analyzed geopotential height as the lateral boundary condition for Φ and integrate the analyzed horizontal wind field to obtain the lateral boundary condition for Ψ, with the constraint that there is no net divergence out of the domain. The upper and lower boundary conditions are the analyzed potential temperature at 925 (1000–850-mb average) and 125 mb (150–100-mb average).

As indicated by Davis (1990), the calculation of PV from (3.2) has errors (induced from random wind and temperature errors) ranging from 0.2 PVU (potential vorticity unit; 10^{-6} m^2 s^{-1} K kg^{-1}) in the lower troposphere to about 1.2 PVU in the lower stratosphere. However, since these are random errors, they may partially cancel when (3.2) is inverted to find the streamfunction and geopotential. Consequently, the balanced flow, which reflects the integral effect of the PV fields, is probably relatively unaffected by random, small-scale noise. In our calculation, we have chosen a threshold for convergence in the inversion of (3.1) and (3.2) so that the balanced solution has a precision of 0.1 m in height and 0.1 m s^{-1} in wind speed.

It should be noted that the inversion scheme tends to break down when the southern boundary is at or south of about 7.5°N. This is probably due to relatively large errors in the analyzed height field near the equator. The imbalance between the mass and wind fields at the southern boundary makes it difficult to obtain a convergent solution. We have tried different methods (e.g., using the wind field to replace the height field) to cope with this problem; however, we have not found a numerical method that successfully inverts PV near the equator. In general, the inversion scheme works when we take 10° or 12.5°N as the southern boundary.

The balanced flow calculated from (3.1) is a nondivergent flow. As described by DE, it is also possible to recover the irrotational horizontal winds (divergent winds) and vertical velocities using an iterative procedure to solve a set of prognostic equations. This method is also adopted in the present study.

2) PIECEWISE PV INVERSION

Piecewise PV inversion represents the process of recovering the balanced flow associated with specific PV perturbations. It is probably the most useful method in the application of PV diagnostics. If the inversion operator is linear, the solutions can be superposed. Piecewise inversion is then simply an application of the method of Green's functions. However, when the balance condition is nonlinear, the solution and its interpretation become much more complicated. Indeed, it has shown that there is no unique solution for nonlinear piecewise inversion (Davis 1992). For these reasons, different methods have been explored/developed for solving nonlinear piecewise PV inversion. [A comparison of three different methods of piecewise PV inversion can be found in Davis (1992).]

In this work, we employ DE's method of piecewise PV inversion, which preserves the symmetry of the inversion process. One important feature of DE's method is that the PV field is partitioned in such a way that the summation of the balanced height and streamfunction fields associated with each individual PV perturbation equals the total balanced fields. In practice, however, we must deal with the influence of the lateral boundary. Though inverting over the entire hemisphere would not require lateral boundary conditions, it is not practical in terms of numerical efficiency. When the PV field is divided into separate PV anomalies, we have no a priori knowledge of the solution at the lateral boundary associated with individual PV anomalies. For this reason, we shall generally use homogeneous lateral boundary conditions in solving the piecewise PV inversion problem (we do not have to worry about the top and bottom boundary conditions because potential temperature perturbations at both of the two boundaries are considered to be part of the PV distribution). For computational efficiency, we wish to choose the domain to be as small as possible. But we need to ensure that the lateral boundary extends at least a few Rossby radii from the region of interest so that the influence of the imposed boundary conditions is minimal. As a compromise, in this study, we choose the domain for piecewise PV inversions to be from 2.5° to 62.5°N and from 120° to 30°W. (Note that because we are using homogeneous boundary condition in solving the piecewise PV inversion, unlike the case of total PV inversion, the piecewise PV inversion works at 2.5°N.)

c. *Potential vorticity partitioning*

1) DEFINING THE MEAN AND PERTURBATION

Defining the mean flow (basic state) for piecewise PV inversion is somewhat arbitrary. It depends upon the purpose of the work. For example, in the study of extratropical cyclogenesis, DE defined a perturbation as the departure from a time average. They chose a typical synoptic-scale wave period (e.g., 5 days) as the time-averaging period.

Hurricanes are intense and isolated vortices with lifetimes much greater than typical synoptic timescales. The motion of tropical cyclones, however, is strongly influenced by their interaction with the nonuniform and evolving background flow. Thus, it is difficult to define a suitable time mean for the study of hurricane motion.

As a first approach, we will construct the 1991 July-to-September time-average flow as our reference state and define deviations from that mean as perturbations. The advantage of this definition is that the mean represents a climatological reference state that permits easy comparisons between different case studies of hurricanes. The shortcoming is that the perturbations thus defined may have little relation to the hurricane itself.

To recover the mean (climatological) balanced flow field, we perform a PV inversion of the total mean PV, using climatological values of Φ, Ψ, and θ as boundary conditions.

2) PARTITIONING OF THE PERTURBATION

Although partitioning the PV perturbations is also somewhat arbitrary, there are at least two classes of perturbations to be considered: one consists of perturbations that are spatially isolated and the other consists of perturbations that are associated with a distinct PV gradient in the mean flow. We seek to divide the PV perturbations into the minimum number of pieces that can efficiently represent the different aspects of hurricane motion. Initially, we will partition the perturbation into two parts: a lower PV perturbation [300 mb and below (including potential temperature perturbations at 925 mb), denoted as L] and an upper PV perturbation [250 mb and above (including potential temperature perturbations at 125 mb), denoted as U]. There are two reasons for such a vertical partition. First, a hurricane generally has a coherent positive PV anomaly in the vertical, extending from the surface to about 300 mb. Second, because there is usually a distinct separation between horizontal PV gradients near the tropopause and PV gradients elsewhere, the upper troposphere is the one of the most "dynamically active" regions. (The other region is near the surface.) We are especially interested in examining the influence on hurricane movement of upper-tropospheric disturbances, which generally exist between 250 mb and the tropopause. From the formulation of the inversion scheme, we know that the total balanced flow should be equal to the summation of the balanced flows associated with the mean PV, L, and U. However, since some midlatitude upper-tropospheric disturbances often extend down to 300 mb or lower, it should be remembered that L can also contain dynamical features that have roots at upper levels. To quantify these, we may also perform piecewise inversion on any significant PV anomaly that we are interested in understanding.

d. Defining the hurricane advection flow

Our aim is to use PV diagnostics to better define hurricane advection (steering) flow. Using the gridded datasets, we interpolate the balanced winds to the center of the hurricane. One significant problem is that when one calculates the balanced wind associated with L, which has a strong azimuthal wind associated with the PV anomaly of the hurricane itself, the resulting interpolated wind is highly sensitive to the exact choice of the hurricane center. To avoid such a problem, we further divide L into two parts: the lower PV of the tropical storm (the positive PV anomalies at 300 mb and below representing the hurricane, denoted as LS), and the remainder (the entire PV anomaly distribution at 300 mb and below, *excluding the hurricane anomaly,* denoted as LE). Typically, LS covers only few grid points.

The balanced flow associated with LS is axisymmetric, as might be expected. We assume that this part of the flow cannot by itself advect the hurricane. We can then avoid the sensitivity problem by defining the hurricane advection flow to be the summation of the balanced flows (at the cyclone center) associated with the mean PV, LE, and U. The hurricane advection flow is thus defined as the balanced flow (at the storm center) associated with the whole PV in the troposphere, except for the PV anomaly of the hurricane itself. In addition, we can also find a point at which the interpolation of the balanced flow associated with the hurricane PV anomaly (LS) is zero. This is one way to better characterize the hurricane center in the analysis. We will refer to such a center (identified from the balanced flow associated with LS) as the *balanced vortex center.*

4. Results

Results from the case study of Hurricane Bob (1991) are presented in this section. The best track positions of this tropical cyclone are displayed in Fig. 1. This storm is chosen for one main reason: It is a recent storm located close to the United States and, thus, to a dense rawinsonde network, suggesting that the quality of NMC analyses for this storm might be better than for a typical storm in the Tropics.

a. Climatology

We have constructed a climatology by taking an Eulerian time (July–September) mean of all dynamical fields [including the (geopotential) height, potential temperature, wind, and potential vorticity fields] in 1991. The isentropic PV distribution (Fig. 2) shows that the climatological PV contours are oriented in the zonal direction. The PV gradient is much more concentrated in the upper troposphere than in the lower and middle troposphere.

Figure 3 shows the climatological mean height and wind fields. A comparison between the mean wind and the mean balanced wind (not shown) indicates that their difference has magnitudes less than 1 m s^{-1} at most places (except perhaps over southeast part of the domain over the North Atlantic Ocean) at 700 mb and less than 2.5 m s^{-1} at 150 mb, except near the boundaries. These differences are within about 15% of the magnitude of the wind and are less than one-half of typical rawinsonde errors [about 3 m s^{-1} in the lower troposphere and 5 m s^{-1} in the upper troposphere (Bengtsson 1976)]. Therefore, the climatological mean state is close to a state of nonlinear balance. The mean wind field shows that upper-level winds are dominated by westerlies. In the lower and middle troposphere, the winds are dominated by easterlies in the tropical region and westerlies in midlatitudes. Also, as shown in Fig. 3, there is a broad anticyclonic circulation over the subtropical Atlantic Ocean associated with the summertime Bermuda high.

This is the background environment the hurricanes are embedded in. We shall use PV diagnostics to understand how individual PV perturbations from this mean state contribute to deflecting storm motion from the mean advection flow.

b. Synopsis of Bob

Our synopsis is primarily based on the Hurricane Preliminary Report from the National Hurricane Center. Hurricane Bob originated from the remnants of a frontal trough just south and southeast of Bermuda on 12 August 1991. The disturbance moved southwestward, became organized over the next few days, and was deemed a tropical depression at 0000 UTC on 16 August near the Bahamas. The depression was upgraded to Tropical Storm Bob later on the same day when it was located about 135 miles northeast of Nassau. The storm then moved northwestward and continued strengthening, reaching hurricane strength on the 17th about 225 miles east of Daytona Beach, Florida. Bob then accelerated, turning toward the north and then north-northeast. Bob continued intensifying and reached its maximum intensity, characterized by 51 m s^{-1} sustained winds and a 950-mb central pressure on the 19th when it was located 100 miles east-southeast of Norfolk, Virginia. The storm weakened while moving to the north-northeast over cooler waters off the mid-Atlantic coast. It made landfall at Newport, Rhode Island, about 1800 UTC on the 19th. Bob next moved across Rhode Island and Massachusetts, while continuing to weaken. The storm made final landfall as a tropical storm near Rockland, Maine, at 0130 UTC 20 August and eventually evolved into an extratropical cyclone over the Gulf of St. Lawrence.

c. An example: 1200 UTC 18 August 1991

We have examined nine different times during the life of Bob, from 1200 UTC 16 to 1200 UTC 20 August

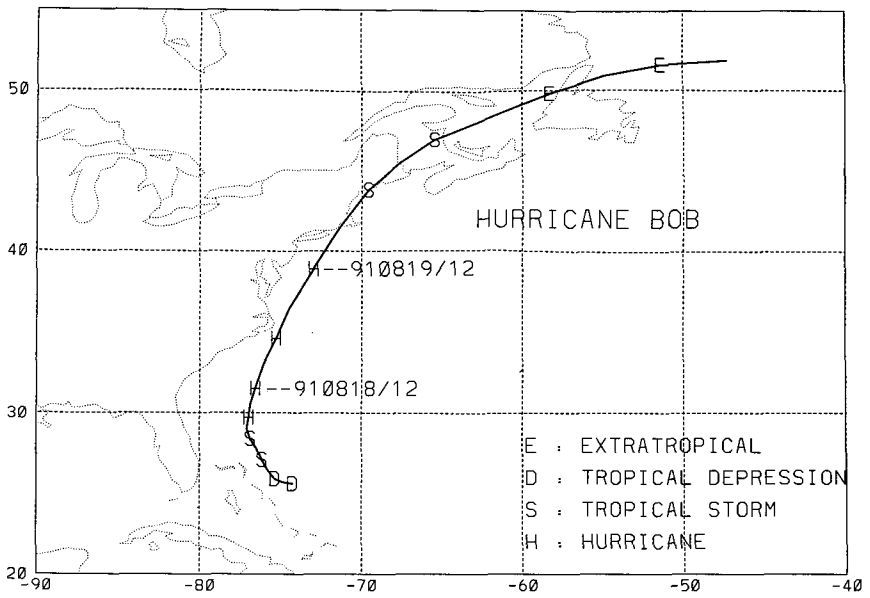

FIG. 1. Best track positions for Hurricane Bob of 1991. The E, D, S, and H indicate the storm position every 12 h.

1991 at 12-h intervals. In this section, we choose one particular analysis time (1200 UTC 18 August 1991, when Bob was located about 170 miles east-southeast of Charleston, South Carolina) to demonstrate the general behavior of the storm, using the NMC analyses.

1) GENERAL FINDINGS

In the relative vorticity field (not shown here) Bob appears as a local maximum with a value near 1×10^{-4} s^{-1} at 850 mb. This local maximum decreases with height and changes sign above 300 mb. A region of negative relative vorticity with values of -4×10^{-5} s^{-1} is observed at 150 mb above Bob. These features are also indicated in the PV field (as shown in Fig. 2 of WEM). The distribution of relative vorticity in the lower troposphere is more uniform than that in the upper troposphere. Except for the strong vorticity values associated with Bob and another system over eastern Quebec, there are no other strong features at 850 mb. But in the upper troposphere (e.g., at 300 mb), many features with large relative vorticity values exist.

Figures 4a and 4b show the NMC analyzed and the balanced height fields. They agree well in most regions, except for some differences over the Atlantic Ocean. Bob is identified as a height minimum in the lower and middle troposphere. The synoptic environment includes a mid- to upper-level trough extending from the southeastern United States beyond the Great Lakes, a subtropical high over the Atlantic, and a strong upper-level ridge east of Canada.

The balanced (nondivergent) wind fields at 700 and 150 mb are shown in Figs. 4c and 4d. A cyclonic flow surrounds Bob at 700 mb with a maximum wind speed of nearly 12 m s^{-1}. This is less than one-third of Bob's actual maximum wind speed. The upper-level trough over the Great Lakes can be seen clearly at 150 mb. This feature is also evident at 700 mb. The difference between the analyzed wind and the balanced wind at either level (not shown here) is small compared with the magnitude of the total wind speed in most places (except over certain areas in the Gulf of Mexico at 700 mb and near the lateral boundary at 150 mb). In general, comparing the balanced heights and winds with the "real" (NMC analyzed) heights and winds, we find that the analyzed data are close to a state of nonlinear balance. This example suggests that there is a close relationship between the analyzed and balanced winds in this region.

As shown above, the comparison of wind, height, and relative vorticity fields from the NMC gridded datasets all indicate that the analyses capture Bob's existence. They also locate Bob's position reasonably well. However, the analyses clearly underestimate Bob's intensity, as measured by maximum winds and minimum pressure, and the strength of its outer circulation. This is partly due to the lack of observations and partly because of the coarse resolution of the datasets causing Bob's structure to be smeared out. This is also the case in Tropical Storm Ana and Hurricane Andrew (Wu and Emanuel 1995). Because of this drawback in the data, we may not be able to accomplish one of our objectives, that is, to understand how a hurricane changes its background environment flow and how these change the subsequent hurricane motion.

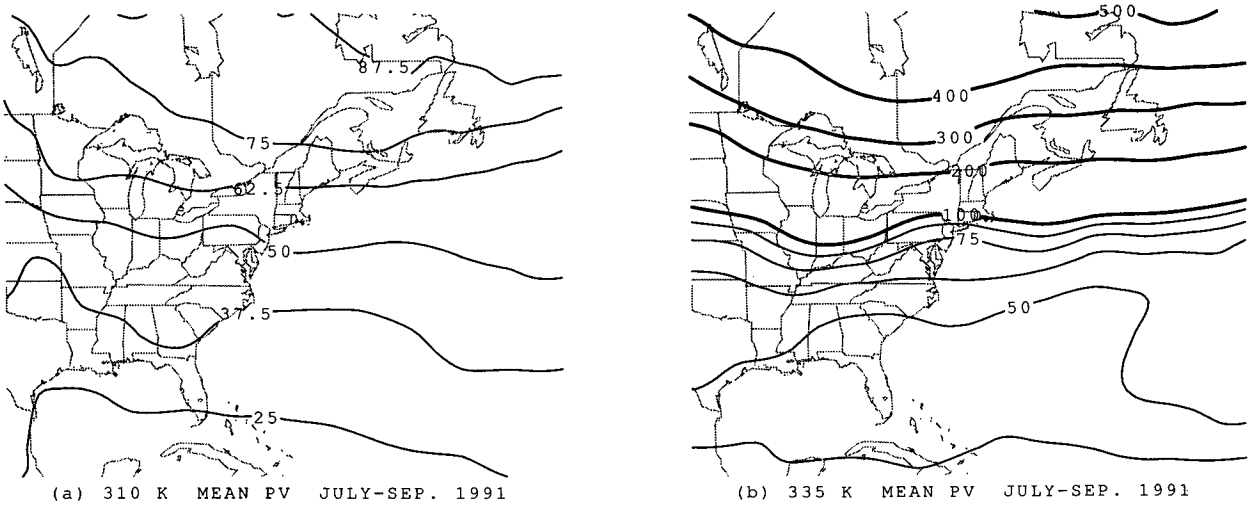

FIG. 2. Mean (July–September 1991) Ertel's potential vorticity fields at (a) 310-K, and (b) 335-K isentropic surfaces. The unit is 0.01 PVU. Potential vorticity values smaller than (larger than or equal to) 1.0 PVU are shown as dashed lines (solid lines) with contour intervals of 0.125 PVU (1.0 PVU).

Piecewise inversion is performed in pressure-like coordinates (Exner function) instead of isentropic surfaces. We plot PV perturbations (relative to the climatological mean) on isobaric surfaces in Fig. 5. Bob appears as a positive PV anomaly in the lower and middle troposphere. At 700 mb Bob is characterized as a positive PV anomaly with a maximum value of 0.4 PVU. Besides Bob, there are some other weaker PV perturbations found in the midlatitudes at this level. At higher levels (e.g., 150 mb) above Bob, however, an area of negative PV anomalies is found, with a tail extending downshear from the storm center. This map is similar to the picture portrayed by the theoretical model of WEM. However, in the real atmosphere, we note that there are also many other distinct PV anomalies, which are neglected in the idealized model (WEM). At 700 mb a negative PV anomaly and a positive PV anomaly are present on the northeast and the southwest sides of Bob, respectively, which look somewhat like the β gyres predicted by barotropic numerical models. However, this cannot be confirmed without studying the time evolution of the PV fields.

As indicated in Fig. 2 of WEM, the magnitude of the horizontal gradient of potential vorticity in the upper

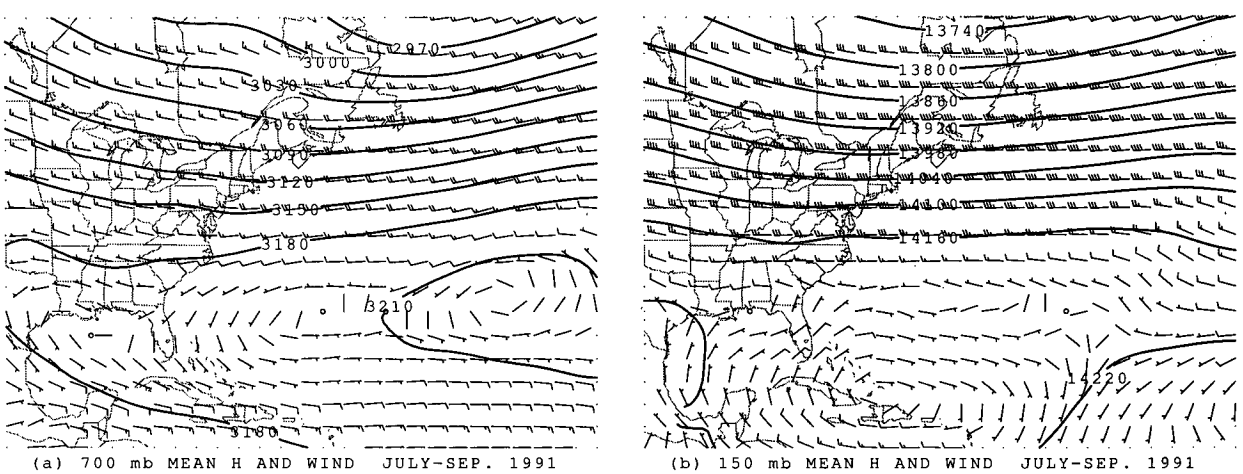

FIG. 3. Mean NMC analyzed height and wind fields at (a) 700 mb, and (b) 150 mb. Contour intervals are 30 m for (a) and 60 m for (b). One long barb indicates 10 knots (8–12 kt); one short barb indicates 5 kt (3–7 kt); no barb indicates winds less than 3 kt; "0" indicates no wind.

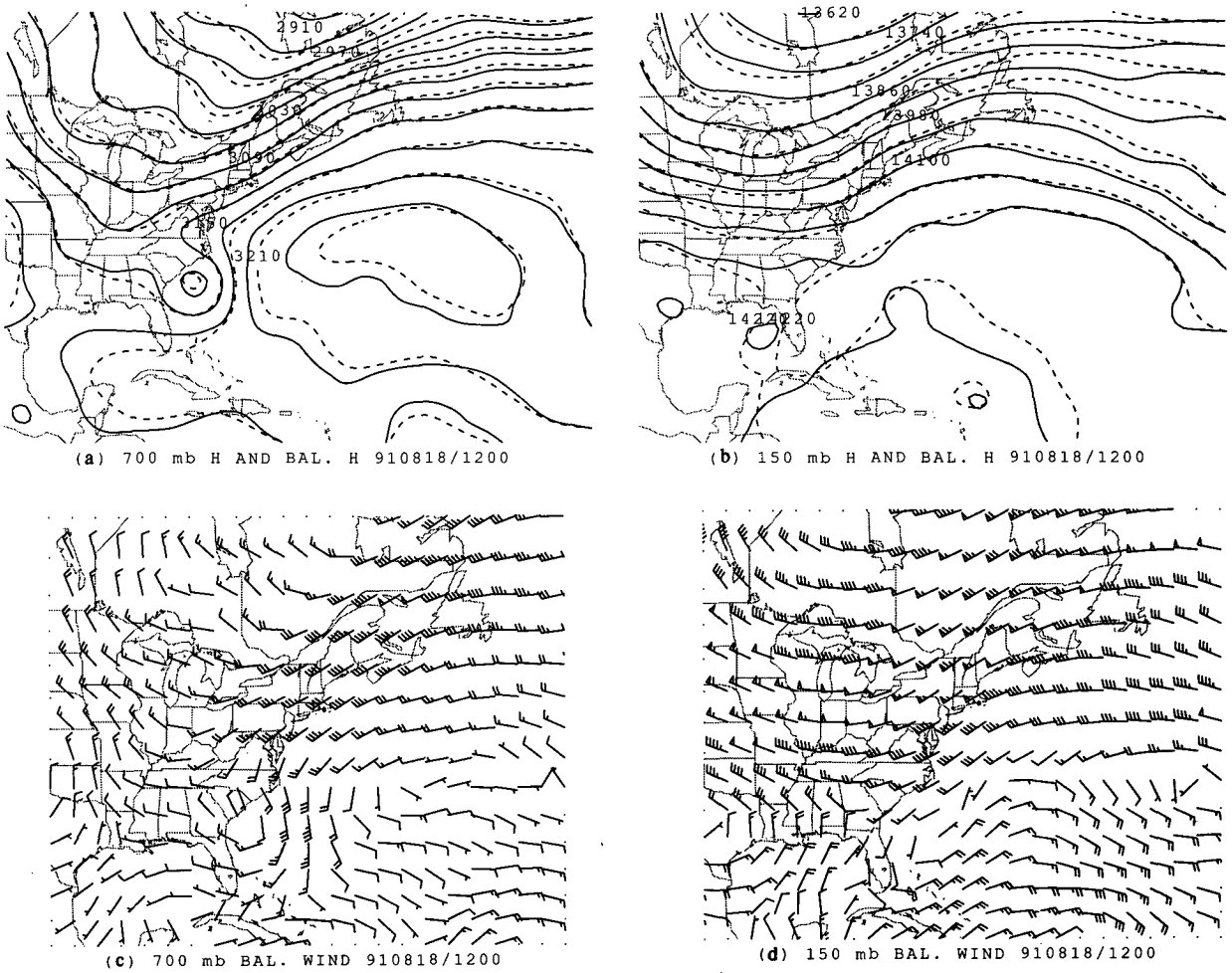

FIG. 4. NMC analyzed height fields (solid) and balanced height fields (dashed) at 1200 UTC 18 August 1991 at (a) 700 mb, and (b) 150 mb. Contour intervals are 30 m for (a) and 60 m for (b). Balanced (nondivergent) wind field (wind barb plotted as in Fig. 3) at (c) 700 mb and (d) 150 mb.

troposphere is much higher than that in the lower and middle troposphere. Figure 5 demonstrates that the amplitude of PV perturbations is also much higher in the upper troposphere than that in the middle and lower troposphere. At 150 mb, in addition to many small-scale PV anomalies, there are two distinct synoptic-scale PV anomalies: a positive PV anomaly associated with the trough over the Great Lakes and a negative PV anomaly associated with a ridge located near Newfoundland. Since these PV anomalies are strong and have a relatively large horizontal scale, their associated geopotential anomalies extend well downward into the troposphere. These features can also be identified in the so-called "dynamic tropopause" potential temperature map (see Fig. 9d). The negative PV anomaly above Bob shows up as a warm potential temperature anomaly, and the aforementioned synoptic-scale positive and negative PV anomalies are manifested by warm and cold potential temperature anomalies, respectively. Since this map concisely depicts the dynamic information in the upper troposphere, for simplicity, we shall use such maps to follow the time evolution of the upper-level systems in our study.

2) ADVECTION FLOW OF BOB

Figure 6 shows the balanced wind field associated with U. In the upper troposphere, there are small-scale cyclonic or anticyclonic circulations in the subtropics, but the large-scale flow field is dominated by a strong circulation dipole in midlatitudes. In the lower and middle troposphere, the flow in the subtropics becomes uniformly easterly. The lower-tropospheric flow field is dominated by the dipole of gyres; a cyclonic circulation associated with a positive upper-level PV anomaly located northwest of Lake Superior and an anticyclonic circulation associated with a negative upper-level PV anomaly over Newfoundland. This result indicates that

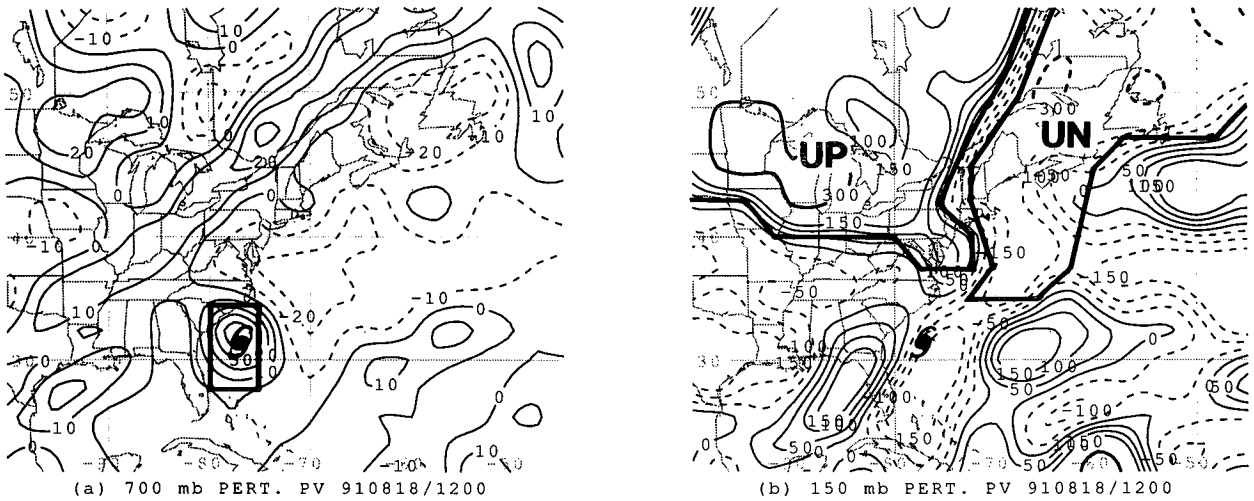

FIG. 5. Ertel's potential vorticity perturbation fields at 1200 UTC 18 August 1991. The unit is 0.01 PVU. Positive (negative) values are represented by solid (dashed) lines. Hurricane Bob's best track positions are indicated by the hurricane symbol. (a) At 700 mb. The contour interval is 0.1 PVU. The area enclosed by heavy lines indicates the potential vorticity anomaly of Bob (LS at 700 mb). (b) At 150 mb. Potential vorticity values smaller than or equal to (larger than) 1.5 PVU are shown as thin lines (bold lines) with contour intervals of 0.5 PVU (1.5 PVU). The area enclosed by heavy lines indicates the potential vorticity anomalies of UP and UN at 150 mb.

the projection of the upper-tropospheric disturbance on the lower troposphere is dominated by the large-amplitude synoptic-scale PV gyres.

In a linear PV inversion (e.g., quasigeostrophic inversion), the penetration depth is determined by an external parameter, fL/N. The aforementioned finding reflects that, as shown in Davis (1992), the vertical penetration depth of a disturbance depends not only on the horizontal scale but also on the amplitude of PV anomalies in a nonlinear PV inversion.

Looking at the vertical distribution of the PV anomalies (not shown here), we find that the two midlatitude PV anomalies are mainly confined between 250 mb and the top of the domain. Next, we conduct a piecewise inversion of each anomaly separately: UP represents the upper-level positive PV anomaly over Lake Superior; UN represents the upper-level negative PV anomaly over Newfoundland. (The PV anomalies of UP and UN at 150 mb are illustrated as the area enclosed by heavy lines in Fig. 5b.) The balanced flow fields associated with UP and UN (not shown) clearly indicate that the circulations associated with these two PV anomalies have a strong component at the subtropics in the lower troposphere. The balanced flow associated

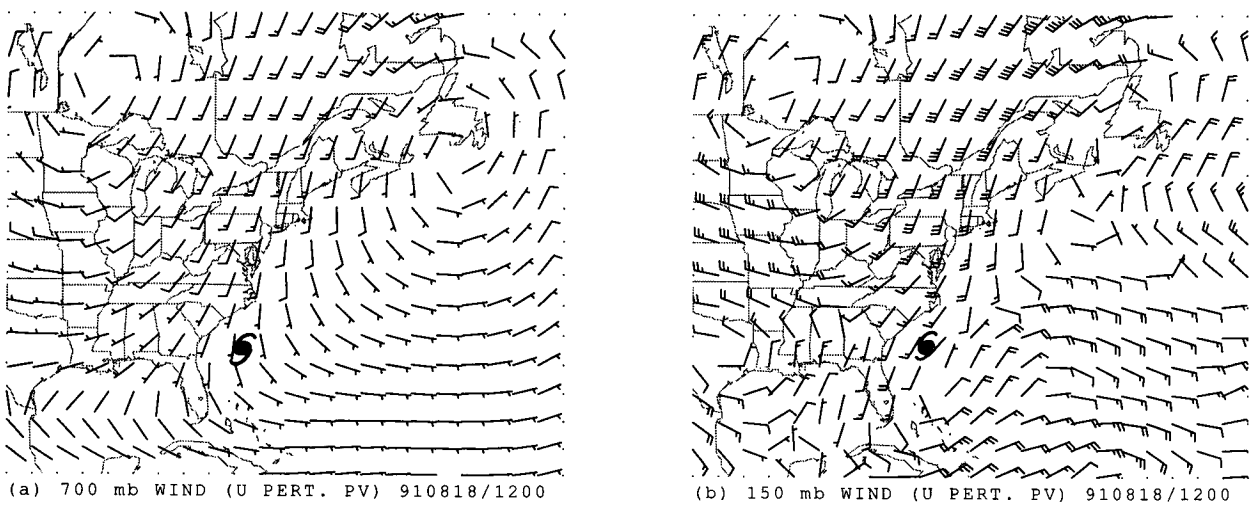

FIG. 6. Balanced wind fields (wind barb plotted as in Fig. 3) associated with potential vorticity perturbation at and above 250 mb (U) at 1200 UTC 18 August 1991 at (a) 700 mb and (b) 150 mb. Hurricane Bob's best track positions are indicated by the hurricane symbol.

with UP would advect Bob 4 m s^{-1} toward the north-northeast, and UN would advect Bob 3 m s^{-1} toward the northwest. If we add these two balanced flows together (UP + UN), the sum is close to that associated with U (Fig. 9a), except that the former has a stronger circulation that extends farther south (e.g., over the Caribbean). The two synoptic systems act to steer Bob northward relative to the climatological flow by about 3 m s^{-1}, which is about 20% higher than for the total U.

We have also performed piecewise inversions of the upper-level anomalies located in the subtropics and the negative upper-level PV anomaly aloft on the downshear side of Bob. The projection of each of these balanced flows at 700 mb is weak (less than 1 m s^{-1}). Also, there is considerable cancellation between the flow fields, making their net contribution to the advection of Bob less significant (less than 1 m s^{-1}). We may conclude that, compared to the midlatitude synoptic-scale PV anomalies, these PV anomalies are dynamically less important in affecting Bob's motion.

Figure 7 shows the balanced flow associated with L. A cyclonic flow surrounds Bob. However, when we invert LE (neglecting the positive PV anomaly near the center of Bob), as shown in Fig. 7b, the cyclonic flow around Bob nearly disappears. We note other rotational flows outside Bob in Figs. 7a and 7b. If we invert the negative PV anomaly found to the northeast of Bob, which might be related to a "β gyre," we find a balanced flow (not shown here) that contributes a 2.9 m s^{-1} southeasterly wind through Bob's center. However, the inversion from other parts of LE tends to counter this wind. Therefore, unlike the large-scale flow fields associated with U (Fig. 6a), there is some cancellation of the flows associated with individual PV features in the lower and middle troposphere that cause the net influence from LE on Bob's movement to be small (less than 0.5 m s^{-1}).

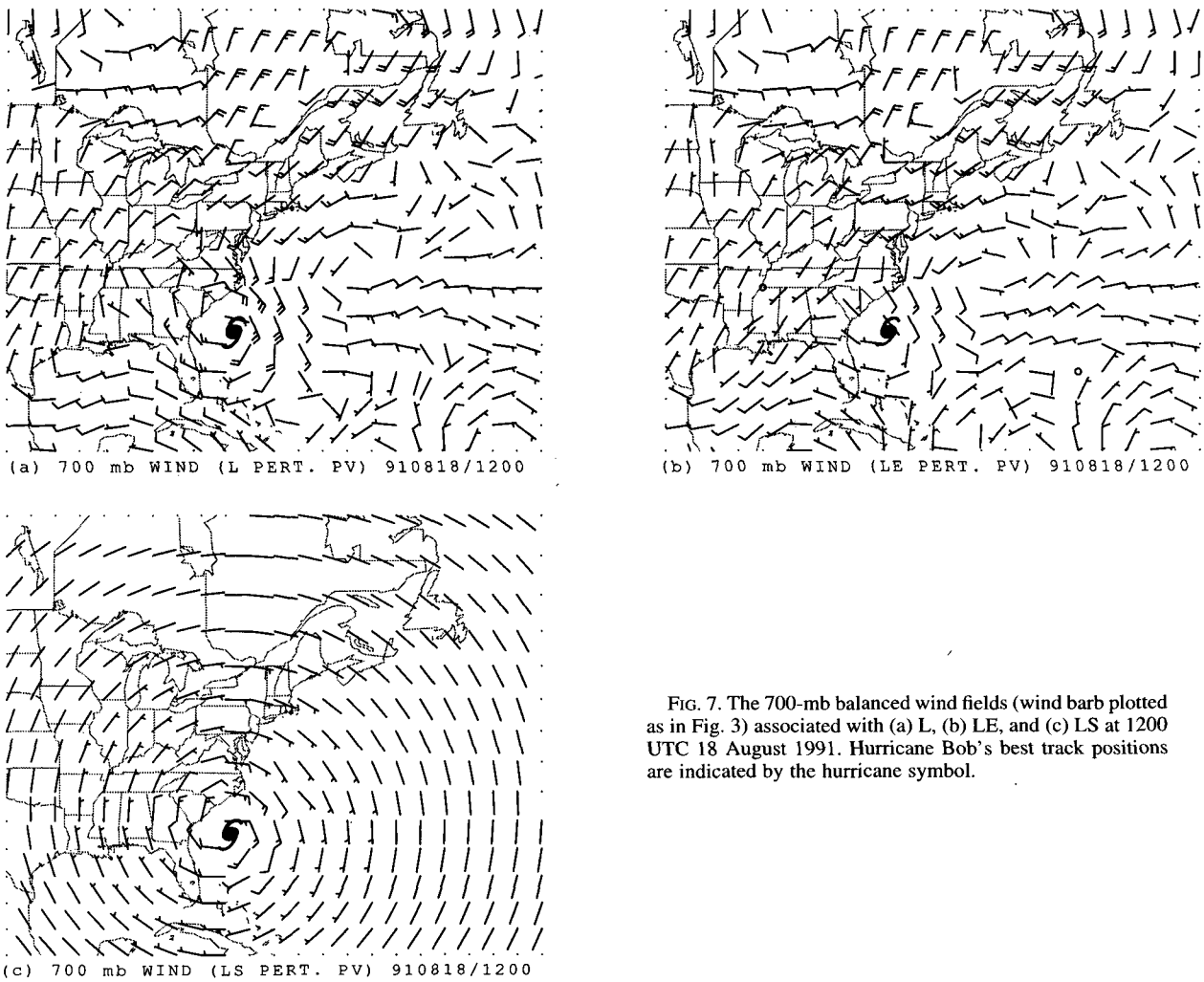

FIG. 7. The 700-mb balanced wind fields (wind barb plotted as in Fig. 3) associated with (a) L, (b) LE, and (c) LS at 1200 UTC 18 August 1991. Hurricane Bob's best track positions are indicated by the hurricane symbol.

The procedure of removing the hurricane PV anomaly (LS) is demonstrated here. In the case of the 700-mb PV perturbation distribution in Fig. 5a, we remove LS in the 12 central grids surrounding Bob (shown as the area enclosed by heavy lines). The process of removing the cyclone's PV anomaly is somewhat subjective. Here, we assume that the advection of the hurricane associated with LS can be neglected. Because any asymmetric features in the removed PV anomalies may actually contribute to the advection of the storm, a better method is to remove the axisymmetric component of the hurricane's balanced flow. However, as indicated in the previous section, since the NMC datasets do not capture detailed flow structure well near the hurricane center, it is not clear whether the asymmetric features in the hurricane center are realistic or not. For this reason, we advocate removing the entire PV anomaly near the hurricane center. To estimate the possible errors induced by this procedure, we perform sensitivity experiments by varying the area containing the actual PV anomaly to be taken out. The results indicate that as long as we remove most of the positive PV anomaly surrounding the hurricane, the process of removing more (or fewer) grid values only affects the hurricane advection flow by a small amount.

We also invert LS. The recovered balanced flow is shown in Fig. 7c. The flow field is axisymmetrically distributed around Bob's center, with a maximum azimuthal wind speed of about 8 m s^{-1}. Indeed, it is possible that we can find a location at which this wind field is minimized (actually near zero). We regard such a location as the storm center, analyzed by the datasets. As indicated in section 3, this center is referred to as the "balanced vortex center." It should be noted that the summation of the balanced flows in Figs. 7b and 7c is equal to that in Fig. 7a.

As pointed out by Smith (1994, personal communication), the flow field associated with LS has its outer circulation that decays relatively slowly, like 1/(radius). This implies a very large kinetic energy and angular momentum associated with the storm, which is regarded as purely a positive PV anomaly (LS). A question may be raised whether such a partitioning of flow field makes sense. In nature, at large radii the influence of the low-level positive PV anomaly gets mostly canceled by the influence of the negative PV anomaly aloft, resulting in little or no anomalous flow. For what we are trying to do, we are only concerned about the near-storm flow, which is dominated by the positive anomaly, and the flow beyond about 1000-km radius is weak in any case.

As discussed in section 3, to define the advection flow of Bob, we interpolate the balanced winds from grid points to the appropriate hurricane center. There are many ways to define the hurricane center, for example, the local maximum in relative vorticity, potential vorticity, or minimum streamfunction, etc. Two definitions are used here: one is the "best track center,"

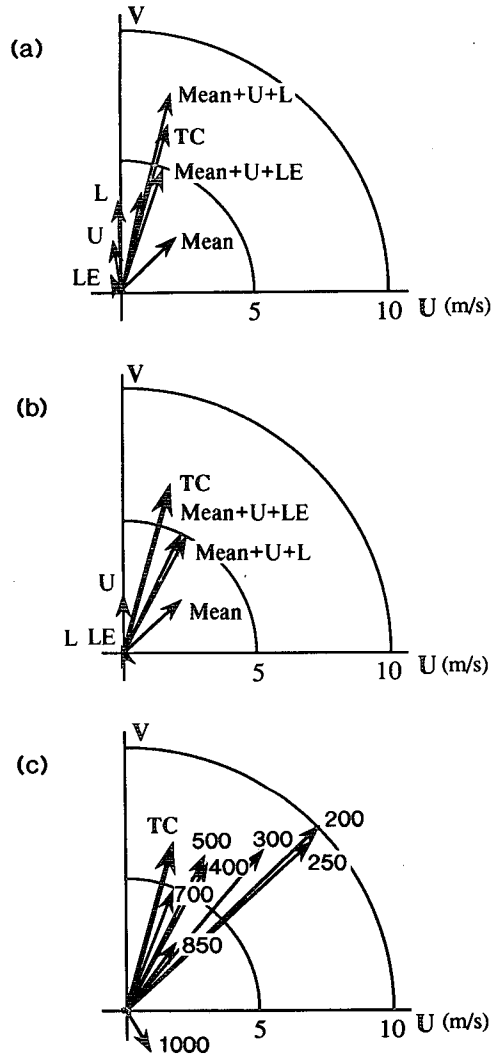

FIG. 8. Velocity vectors of balanced flows and Hurricane Bob's motion at 1200 UTC 18 August 1991. Mean, U, L, and LE represent the 850–500-mb pressure-averaged balanced flows associated with the mean potential vorticity and potential vorticity perturbations of U, L, and LE, respectively. Mean + U + LE represents the total hurricane advection flow; TC indicates Bob's motion estimated from every 6-h best track position. Interpolation of the balanced wind fields (a) to the best track center and (b) to the 850–500-mb pressure-averaged balanced vortex center. (c) Velocity vectors of total advection flow (interpolated to the 850–500-mb pressure-averaged balanced vortex center) at each level.

that is, the storm center analyzed from the National Hurricane Center's postseason analyses using all of the information available, and the other is the "balanced vortex center" (described in section 3) that minimizes the 850–500-mb averaged balanced flow associated with LS.

Figures 8a and 8b show a comparison of the 850–500-mb pressure-averaged balanced flow (interpolated to the hurricane center) with the actual hurricane motion at 1200 UTC 18 August. In this example, Bob's

best track position is at 31.5°N, 76.6°W, and the balanced vortex center is located at 31.62°N, 77.48°W. The two centers differ by about 1° longitude. After interpolation, the balanced flows associated with U and the climatological mean are about the same for either center. However, the balanced flow associated with L is different for the two centers. This is the sensitivity problem we mentioned in section 3. As we have neglected the wind field associated with the hurricane PV, we get the balanced flow associated with LE. Again, it is about the same for the two different centers (note that when we use balanced vortex center for interpolation, by definition, the balanced flow associated with L and LE are identical at the balanced vortex center).

When we sum the balanced flows associated with mean, U, and LE, we recover the 850–500-mb pressure-averaged advection flow for Bob. Figures 8a and 8b indicate that the advection flows using the two different interpolated centers are about the same. (Hereafter, we only show the result of the advection flow that is interpolated to the 850–500-mb pressure-averaged balanced vortex center.) Moreover, these advection flows give a good estimate of the direction of Bob's motion (north-northeastward), though the magnitude is about 1 m s^{-1} less than Bob's displacement speed (6.6 m s^{-1}). It should be noted that the actual storm motion is estimated by averaging the previous and subsequent 6-h mean motion, calculated using the 6-h best track positions. Given an error of 0.1° for the best track positions, this estimation of the cyclone motion has a potential error of about 1 m s^{-1} in magnitude. Also, with the PV analyses, we are making a local (in time) estimate of advection speed. But the actual storm motion may vary in time.

It can also be seen that Bob's movement is due not only to the climatological mean balanced flow but to significant contributions from the balanced flow associated with the upper-tropospheric PV perturbations (U). Two points emerge. First, Bob's motion is being strongly influenced by the midlatitude systems. Second, disturbances in the upper troposphere play an important role in advecting Bob.

The preliminary report of Bob from the National Hurricane Center describes that, around this time, Bob began turning toward the north and then north-northeast at an increasing forward speed and that its motion was mainly due to the combined effect of the subtropical high pressure ridge over the Atlantic and a mid- to upper-level trough over the southeastern United States. Compared with our findings, the former flow feature appears to be an effect of the climatological mean balanced flow. Based on this analysis, the conjecture regarding the trough over the southeastern United States is probably incorrect. To show this, we also inverted the upper-level PV anomaly associated with the trough over the southern United States. Since it has a narrow horizontal scale, its projection onto the flow of the lower troposphere is weak, and it is not a primary factor in Bob's movement. As discussed previously, the flow associated with the synoptic-scale upper-level trough and ridge over the Lake Superior and Newfoundland advected Bob. Thus, through PV diagnostics, we are able to distinguish clearly which dynamical features are most important in advecting the cyclone.

Figure 8c indicates the hurricane advection flow (interpolated to the 850–500-mb averaged balanced vortex center) at each level. In general, the flows between 700 and 400 mb are all close to the actual hurricane motion vector. Higher deviations occur at 1000 mb and above 400 mb. Figure 8c also demonstrates that there is a west-southwesterly vertical shear of about 5 m s^{-1} between 700 and 200 mb over Hurricane Bob. We also find (not shown here) that advection flows using a single-level wind (e.g., 700 mb) or over a deeper part of the troposphere (850–300 mb) also approximate the storm movement fairly well. However, in this work, we will generally use the 850–500-mb pressure-averaged flow to represent the hurricane advection flow.

d. Time evolution of Bob

1) EVOLUTION OF UPPER-LEVEL PV ANOMALIES

As the previous example indicates, upper-level PV anomalies are important in influencing Bob's motion. Therefore, to understand the dynamics of Bob's motion, it is desirable to understand the evolution of the upper-level PV perturbations. For Bob, the most important upper-tropospheric PV anomalies are located above 300 mb.

To simplify visualization, we use the potential temperature θ perturbation fields on the dynamic tropopause (surface of 1.5 PVU) to represent disturbances in the upper troposphere. Because of the quasi-conserved nature of both PV and θ, it is convenient to use such maps to trace important features that contain valuable dynamic information in the upper troposphere. It should be also restated that a warm (cold) anomaly on the dynamic tropopause is equivalent to a negative (positive) PV anomaly on an isentropic surface in the upper troposphere (unlike for the lower boundary). Figure 9 shows a time series of such potential temperature anomaly maps from 17 to 20 August. The 700-mb balanced flow field associated with the PV perturbations in the four upper levels (U) are displayed in Figure 10.

At 0000 UTC 17 August (Fig. 9a), a cold anomaly (referred to as C1) is found over South Dakota. Another cold anomaly (C2) extends along the southeastern United States. A warm anomaly (W1) is located over Lake Superior, and another warm anomaly (W2) is found over the northwestern Atlantic. The balanced flow associated with U at 700 mb (Fig. 10a) indicates that Bob is advected by a weak southeasterly wind with magnitude of 1.4 m s^{-1}, mainly associated with W2. The upper-level features, without much change in in-

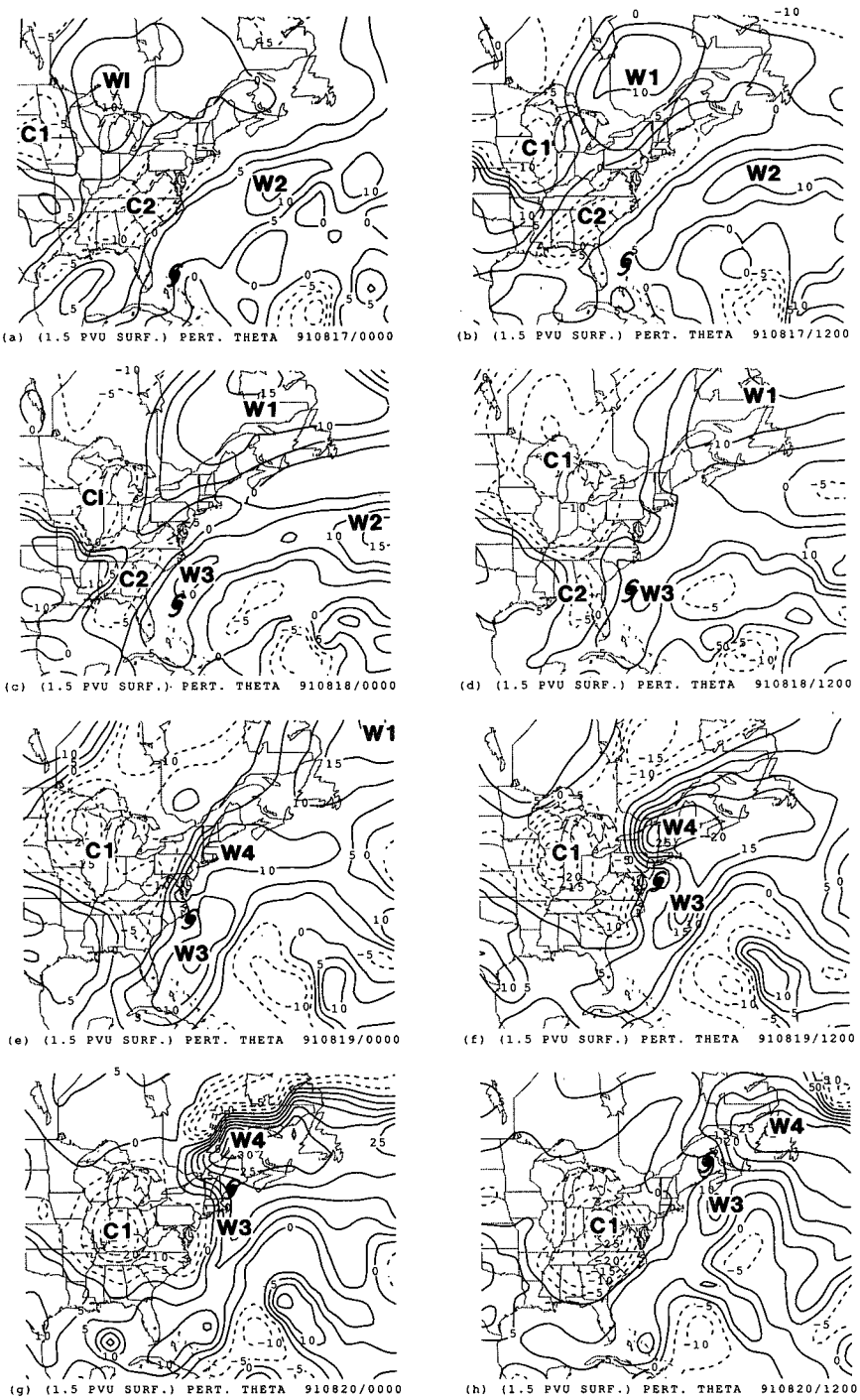

FIG. 9. Time evolution of the tropopause potential temperature perturbation fields (on the 1.5 PVU surface) from 0000 UTC 17 to 1200 UTC 20 August 1991. (a) 0000 UTC 17, (b) 1200 UTC 17, (c) 0000 UTC 18, (d) 1200 UTC 18, (e) 0000 UTC 19, (f) 1200 UTC 19, (g) 0000 UTC 20, and (h) 1200 UTC 20 August 1991. The contour interval is 5 K. All positive (negative) values are represented by solid (dashed) lines. Hurricane Bob's best track positions are indicated by the hurricane symbol.

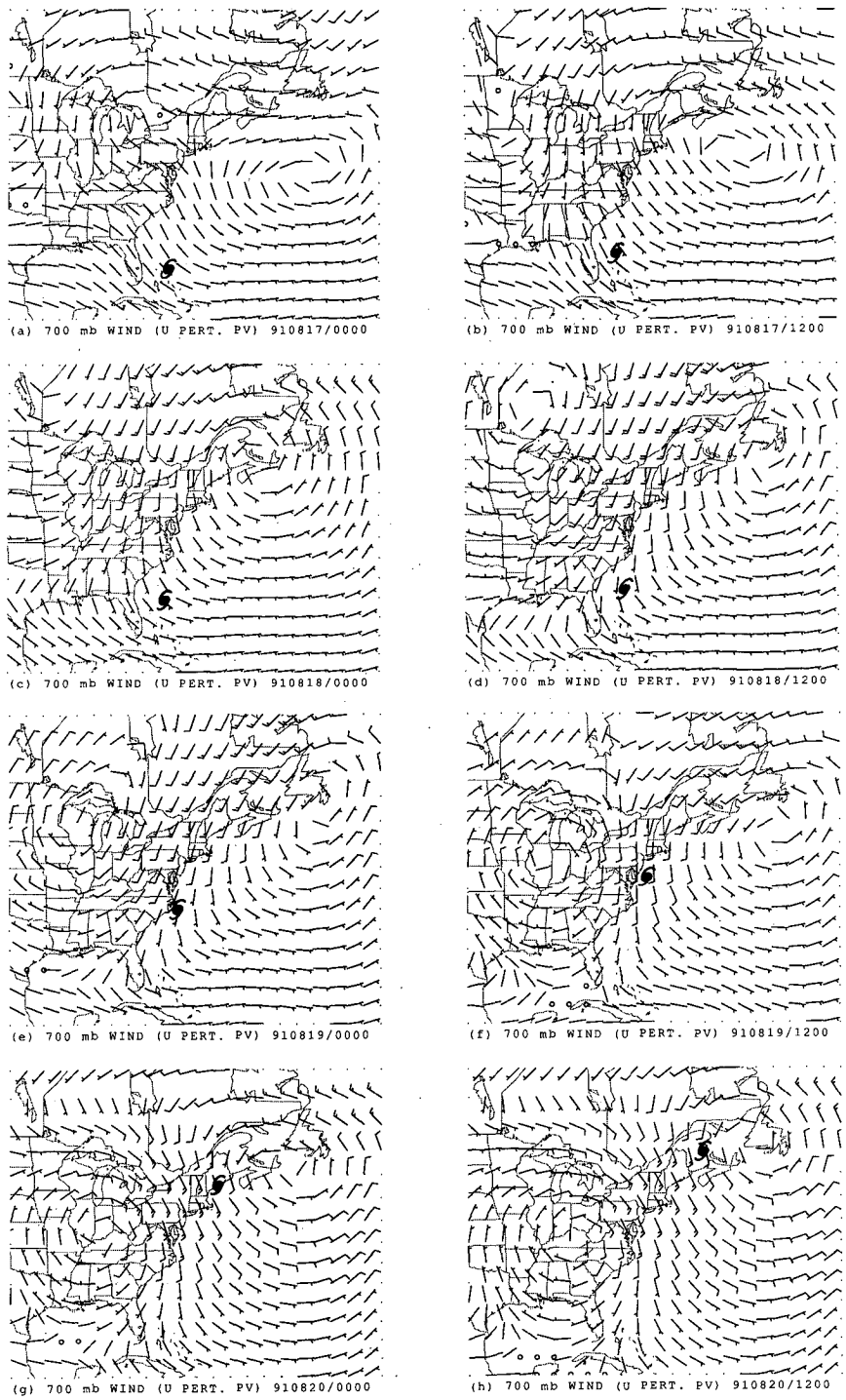

FIG. 10. Time evolution of the 700-mb balanced wind fields (wind barb plotted as in Fig. 3) associated with U from 0000 UTC 17 to 1200 UTC 20 August 1991. (a) 0000 UTC 17, (b) 1200 UTC 17, (c) 0000 UTC 18, (d) 1200 UTC 18, (e) 0000 UTC 19, (f) 1200 UTC 19, (g) 0000 UTC 20, and (h) 1200 UTC 20 August 1991. Hurricane Bob's best track positions are indicated by the hurricane symbol.

tensity, are advected eastward for the next 12 h (Fig. 9b). The flow field (Fig. 10b) shows that Bob is advected by about the same amount of balanced flow associated with the same PV anomaly (W2).

By 0000 UTC 18 August (Fig. 9c), C1 moves farther southeastward, and C2 weakens over the southeastern states. Also, W1 intensifies and expands over southeastern Canada and W2 moves close to the eastern boundary in the domain while intensifying. At this time, a new warm anomaly (referred to as W3) is found near the east coast of North and South Carolina. There is some evidence (see section 2 below) that Bob contributes to the generation of a part of W3. Figure 10c indicates that Bob is advected northwestward at this time by a weak balanced flow of 1.3 m s^{-1}, which is partly associated with W1.

Twelve hours later (Fig. 9d), another cold anomaly is advected southward from Hudson Bay and merges with C1. The new C1 covers the central United States and Canada, centered slightly north of Lake Superior, and connects with C2 having a small tail extending to the west of Florida. Warm anomaly W1 continues to intensify, with its center located over the southeast coast of Canada, while W3 is quasi-stationary. As indicated in the previous section, the balanced flow (Fig. 10d) that advects Bob at this time is mainly associated with the dipole gyres, C1 and W1, that combine to advect Bob northward with a speed of 2.3 m s^{-1}.

By 0000 UTC 19 August (Fig. 9e), C1 has strengthened and moved southward with its center over west Wisconsin. The southern part of C2 is sheared out, and the northern end of C2 merges with C1. Warm anomaly W1 is at the same location with little increase in intensity while W3 has strengthened and is located to the southeast of Bob. Interestingly, another warm anomaly (referred to as W4) forms and is located downshear of Bob. The 700-mb balanced flow (Fig. 10e) exhibits a southerly flow of 2.5 m s^{-1} through Bob's center. This flow is mainly associated with C1, W1, and W4.

After another 12 h (Fig. 9f), C1 has further intensified. It moves southeastward to near north Illinois. Meanwhile, most of W1 has moved out of the domain. However, the magnitude of W4 has increased dramatically to 25 K. It also covers a much larger area. Anomaly W4 is centered over New Hampshire and extends eastward. The associated flow field (Fig. 10f) indicates a dipole of strong gyres associated with C1 and W4. This flow advects Bob northward at 5.5 m s^{-1}.

By 0000 UTC 20 August (Fig. 9g), C1 has moved slightly southeastward. Anomaly W3 further strengthens and extends from southeast Quebec to the eastern boundary of the domain. At this time, the magnitude of the influence of U on Bob's motion reaches its peak. As indicated in Fig. 10g, this flow advects Bob north-northwestward at 6.8 m s^{-1}. This flow field is clearly dominated by C1 and W4. Finally, at 1200 UTC (Fig. 9h), C1 and W4 both move to the east, and their intensities are unchanged. Figure 10h shows that the flow pattern is still mainly associated with C1 and W4, which advects Bob northward with a wind speed of 5.4 m s^{-1}.

2) Upper-level negative PV anomaly above Bob

To compare our findings with WEM's hypothesis discussed in section 2, we discuss the evolution of the negative PV anomaly above Bob. As shown in Fig. 9, at 0000 UTC 17 August, there is no obvious anomaly directly above the location of the storm and it is not clear what relationship the warm anomaly extending northeastward from Bob has to the storm. However, 1 day later, at 0000 UTC 18 August, a warm anomaly of 10 K (W3) forms above Bob and extends to the northeast side of Bob. It remains so for the next 12 h. At 0000 UTC 19 August, when Bob is still intensifying and moving along the east coast of Virginia, W3 extends from the south to the east of Bob with a maximum amplitude of 15 K. Meanwhile, another warm anomaly (W4) forms over Massachusetts, having a maximum amplitude of 15 K, and extends eastward.

The neighborhood of the storm is atypical at this point. Bob is already headed toward midlatitudes where it can readily induce upper-level PV anomalies through horizontal advection, as opposed to vertical transport by nonconservative processes. As Bob moves northward, this warm anomaly (W4) always "follows" Bob, while its amplitude increases from 15 K on 19 August to 30 K at 1200 UTC 20 August, when Bob is located over eastern New Brunswick. This could be either a "phase locking" of the upper-level and lower PV anomalies or the production of negative PV anomaly by Bob. Similar results are found by looking at negative PV anomalies on the 355-K surface (not shown here).

It should be noted that these warm anomalies could intensify because air is moving toward a region having a lower mean θ. However, if we follow the actual θ field on the dynamic tropopause (not shown here), we observe that only θ of W3, but not W4, increases with time in a Lagrangian sense. This result suggests that the early phase of W3 is due to the diabatic process associated with Bob, where as the development to the north (W4) is caused by two dynamic processes: one is the advection of thermal gradients at the tropopause by the flow associated with the lower-level positive PV anomaly of Bob and the other is the downshear transport of the low-PV air, diabatically generated above Bob, by the upper-level ambient flow. Because the NMC analyses underestimate Bob's intensity, we cannot distinguish between the two possible dynamic processes by advecting the PV fields using Bob's associated balanced flow.

Since during these few days Bob was located near the coastal area, we think that the analysis of these PV anomalies is realistic. We could perform piecewise PV inversions to understand how these negative PV anomalies interact with Bob. However, to prove or disprove our hypothesis in the modeling work, we need to be able to identify which PV anomalies observed in the data are generated by diabatic processes near the hurricane center. The best we can do is to follow the evolution of the PV field and trace the change of the PV anomalies. It is difficult to distinguish clearly which part of the anomaly is generated by the hurricane and which parts are due to horizontal advection from other regions. Thus, we shall address this somewhat speculatively.

A simple, preliminary analysis is performed by inverting the U negative PV anomaly (denoted as UNA, which includes W3 and W4) found above and downshear from the location of Bob, which we believe may be a negative PV plume either diabatically or dynamically (through the horizontal advection) produced by Bob. Figures 11a and 11b display the 200-mb PV anomaly areas chosen for inversion at 1200 UTC 18 and 19 August, respectively. The inverted balanced flow fields at 700 mb are shown in Figs. 11c and 11d. On 18 August, the balanced flow through Bob's center is 0.9 m s^{-1} to the north. However, on 19 August, it has increased to a northwestward flow at 4 m s^{-1}, in a direction to the left of the mean southwesterly vertical shear (will be shown later), as predicted by our theo-

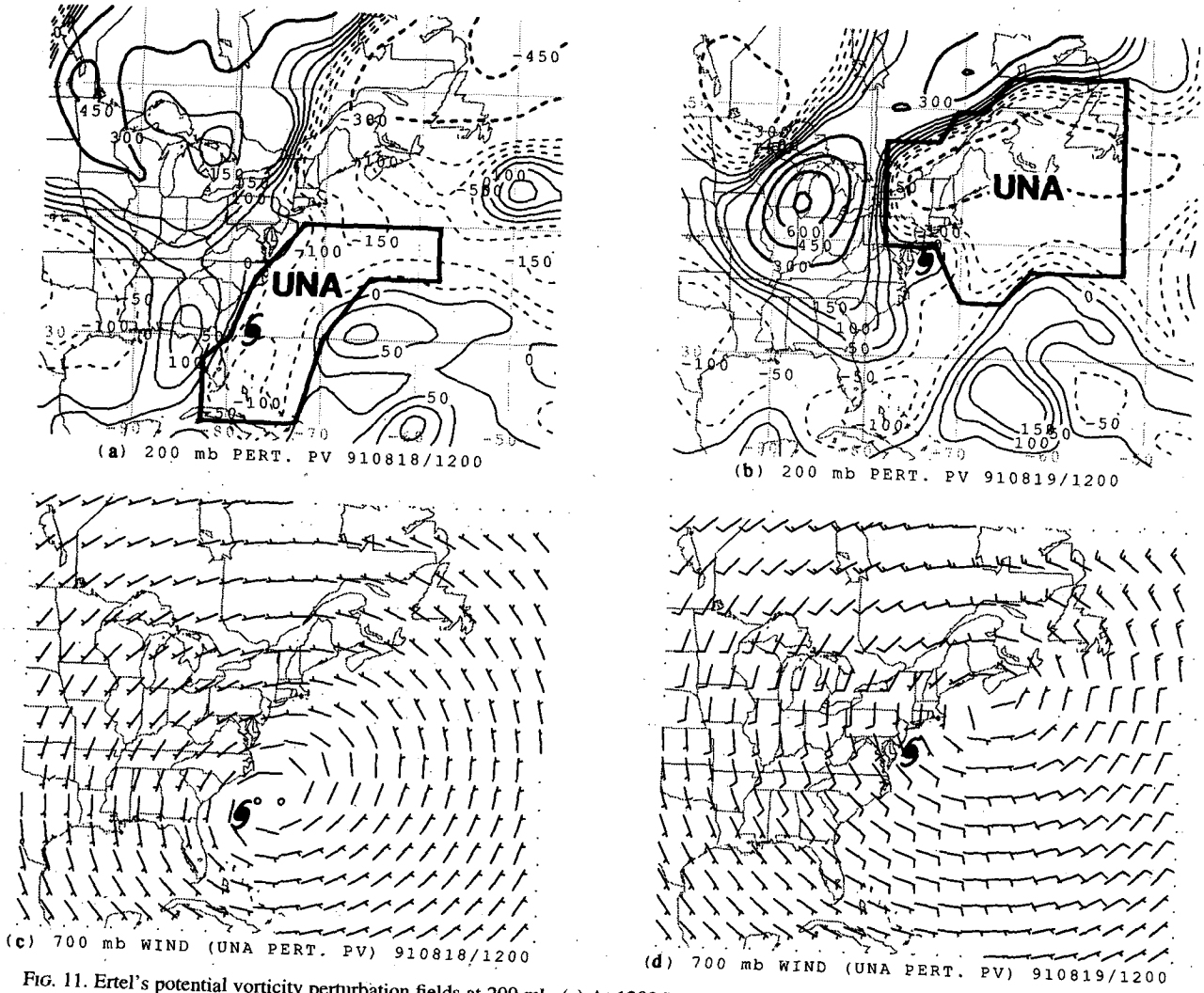

FIG. 11. Ertel's potential vorticity perturbation fields at 200 mb. (a) At 1200 UTC 18 August 1991 and (b) at 1200 UTC 19 August 1991. The area enclosed by heavy lines indicates the potential vorticity anomaly (UNA at 200 mb) to be inverted. The unit is 0.01 PVU. Potential vorticity values smaller than or equal to (larger than) 1.5 PVU are shown as thin lines (bold lines) with contour intervals of 0.5 PVU (1.5 PVU). All positive (negative) values are represented by solid (dashed) lines. The 700-mb balanced wind fields (wind barb plotted as in Fig. 3) associated with UNA. (c) At 1200 UTC 18 August 1991 and (d) at 1200 UTC 19 August 1991. Hurricane Bob's best track positions are indicated by the hurricane symbol.

retical model. Piecewise inversions of W3 and W4 at the 19th are also performed, separately. The result shows the advection flow of Bob is mainly associated with W4. The influence from W3 is relatively weak.

In summary, we find that as the strength of the negative PV anomaly aloft intensifies with time, its effects on advecting Bob also become stronger. Though we are not sure how much of the upper-level PV anomalies are diabatically produced by Bob, by following the evolution of the PV field, we believe that the strengthening of the negative PV anomaly aloft is closely related to Bob. It is not clear, however, whether dynamic or diabatic processes are the main cause of W3 and W4. Thus, our preliminary analysis does not exhibit enough evidence to support WEM's hypothesis. More detailed work needs to be done to evaluate this effect more quantitatively.

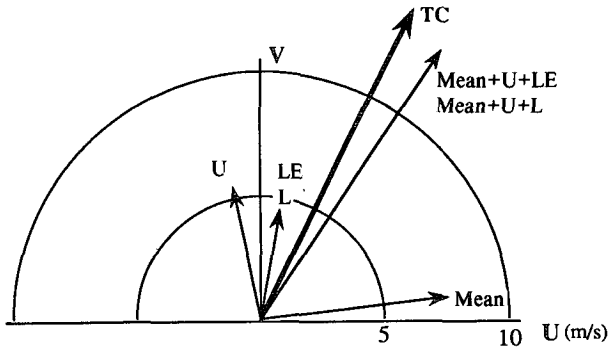

FIG. 12. Velocity vectors of balanced flows (interpolated to the 850–500-mb pressure-averaged balanced vortex center) and Hurricane Bob's motion at 1200 UTC 19 August 1991. Mean, U, L, and LE represent the 850–500-mb averaged balanced flow associated with mean potential vorticity, potential vorticity perturbations of U, L, and LE, respectively. Mean + U + LE represents the total hurricane advection flow. TC indicates Bob's motion estimated from every 6-h best track position.

3) EVOLUTION OF LOWER- AND MIDLEVEL PV ANOMALIES

The 700-mb balanced flow associated with LS (not shown here) is nearly axisymmetric around Bob. Its magnitude becomes stronger with time, though always considerably weaker than the actual wind speeds of Bob.

The evolution of the 700-mb balanced flow associated with LE is studied. Unlike the balanced flow associated with U (Fig. 10) or LS, this flow field (not shown here) has more detailed small-scale features, and there is some cancellation between the flows associated with different PV anomalies. Thus, it is not clear what the dominant dynamic feature is that advects Bob. In general, these balanced flows have about the same magnitude ($1-2$ m s^{-1}) near Bob's center as those associated with U. Interestingly, at 1200 UTC 19 August, as Bob moves rapidly toward the north-northeast, the effect of U increases dramatically, advecting Bob northward by a wind speed of 5.5 m s^{-1}. Meanwhile, the advection by LE increases to a 4.5 m s^{-1} northward flow.

To demonstrate how each component of the 700-mb balanced flow contributes to Bob's motion at 1200 UTC 19 August, we display hodographs of the advecting flow in Fig. 12. The eastward component of Bob's movement at this time is mainly due to the climatological mean flow. The PV perturbations (U and LE) in the upper and lower troposphere play about the same role in advecting Bob toward the north. The sum of the balanced flows is a good approximation to Bob's actual motion at this time.

4) β GYRES

From 18 August on, a lower-level negative PV anomaly is consistently found to the east-northeast of Bob; this anomaly looks somewhat like the negative branch of β gyres. We invert these negative PV anomaly features, located between the surface and 300 mb, at two different times: 1200 UTC 18 August and 1200 UTC 19 August. The PV anomalies at 700-mb to be inverted (denoted as LB) are illustrated in Figs. 13a and 13b, and the balanced flows associated with these PV anomalies are shown in Figs. 13c and 13d. On 18 August, the associated flow tends to advect Bob toward the north-northwest at 2.9 m s^{-1}. However, because of the cancellation with the balanced flow associated with other lower-tropospheric PV anomalies, the net effect of LE on Bob's motion is a northward speed of 0.5 m s^{-1}. On 19 August, the balanced flow acts to advect Bob northward at 3.5 m s^{-1}. Unlike on the 18th, this negative PV anomaly contributes about 80% of the net advecting flow associated with LE.

One may ask how closely the negative PV anomalies are related to so-called β gyres. The location of the anomalies relative to the hurricane and its induced storm drift agree well with the predictions of barotropic theory. However, observations do not show any sign of the additional counterpart in the β gyres, that is, the positive PV anomaly located to the southwest of the storm (it is possible that this positive PV anomaly is mixed in with Bob and cannot be distinguished in the data). Also, given that the data underestimate Bob's strength, it is not clear whether such a negative PV anomaly could be generated by the advection of the background PV gradient (Fig. 2) by the cyclonic circulation associated with Bob. A strong circulation might make this more likely.

To explore this, we calculated the advection of the mean PV field by the balanced flow associated with Bob's PV anomaly (LS) at 18 August and 19 August. The analysis (Fig. 14) indicates that at 0000 UTC 18 August, the relatively weak flow associated with Bob results in negative PV advection to the east of Bob and positive advection to the west. The magnitude of these

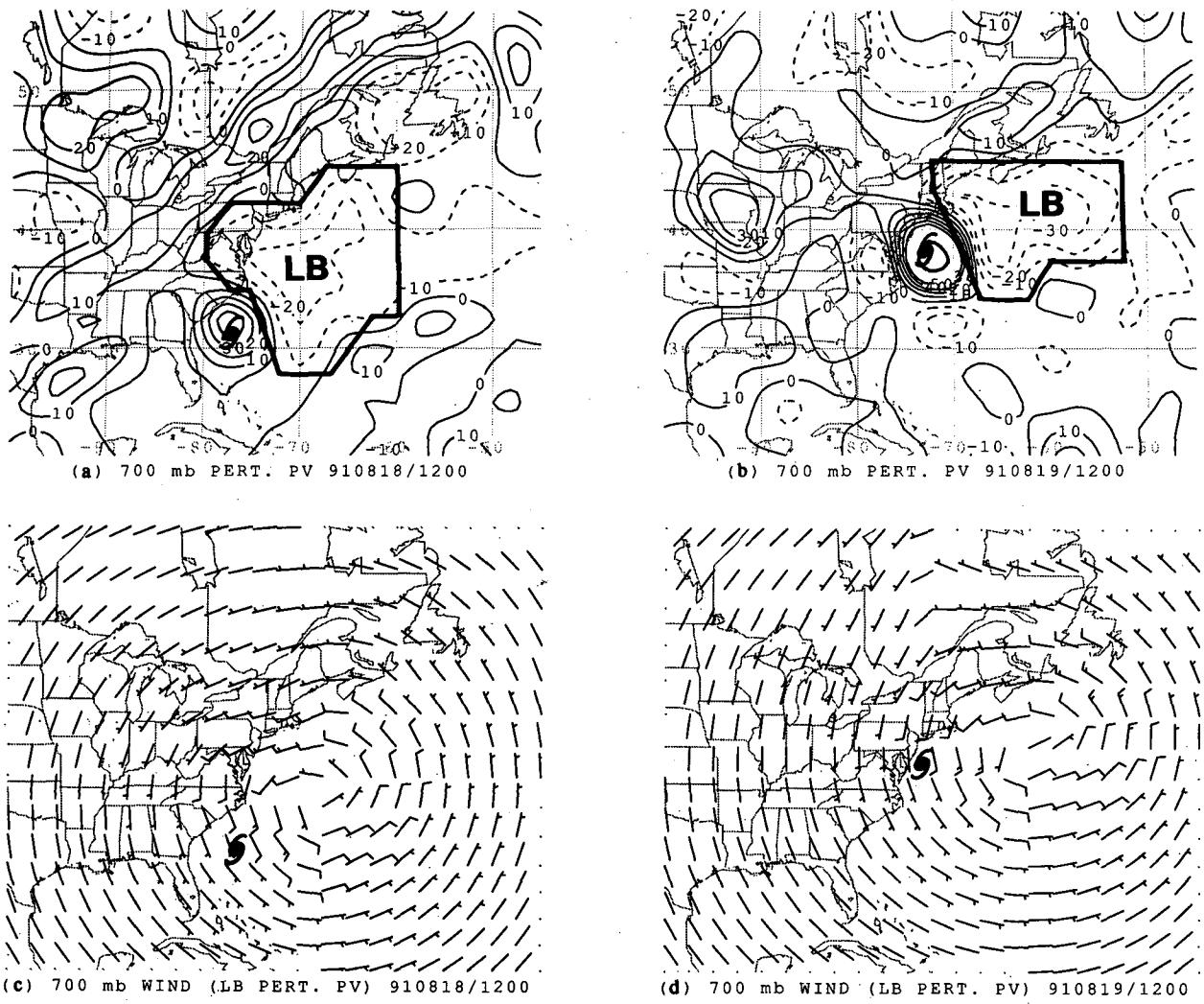

FIG. 13. Ertel's potential vorticity perturbation fields at 700 mb. (a) At 1200 UTC 18 August 1991 and (b) at 1200 UTC 19 August 1991. The area enclosed by heavy lines indicates the potential vorticity anomaly (LB) to be inverted. The unit is 0.01 PVU. Potential vorticity values smaller than or equal to (larger than) 0.5 PVU are shown as thin lines (bold lines) with contour intervals of 0.1 PVU (1.0 PVU). All positive (negative) values are represented by solid (dashed) lines. The 700-mb balanced wind fields (wind barb plotted as in Fig. 3) associated with LB. (c) At 1200 UTC 18 August 1991 and (d) at 1200 UTC 19 August 1991. Hurricane Bob's best track positions are indicated by the hurricane symbol.

PV advections is small, however, with a maximum rate of about 0.05 PVU per 12 h. The PV advection magnitudes increase as Bob's associated winds get stronger. From 0000 to 1200 UTC 19 August, PV advection magnitudes increase from 0.1 to 0.15 PVU per 12 h. Comparing the structure and magnitude of the PV advections with the evolution of the 700-mb PV anomalies (e.g., Figs. 13a,b), however, we do not believe that these perturbations are related to the so-called β gyres.

Thus, we find little evidence of the so-called β effect in our analysis. But, in reality, Bob's outer winds may be stronger, giving more potential for such an effect (though the horizontal PV gradients in the basic tropospheric flow are relatively weak). It should be noted that the NMC analyses may not have a horizontal resolution good enough to resolve β gyres (Reeder et al. 1991). Also, as pointed out by Reeder et al. (1992), it is not certain how to meaningfully partition the hurricane vortex, vortex-induced asymmetries, and the vortex environment. Nevertheless, our observational analysis is unable to confirm whether such an effect occurs. More work needs to be carried out to quantify this effect.

e. Advection flow of Bob

Figure 15 shows the vector differences between the 850–500-mb pressure-averaged calculated advecting

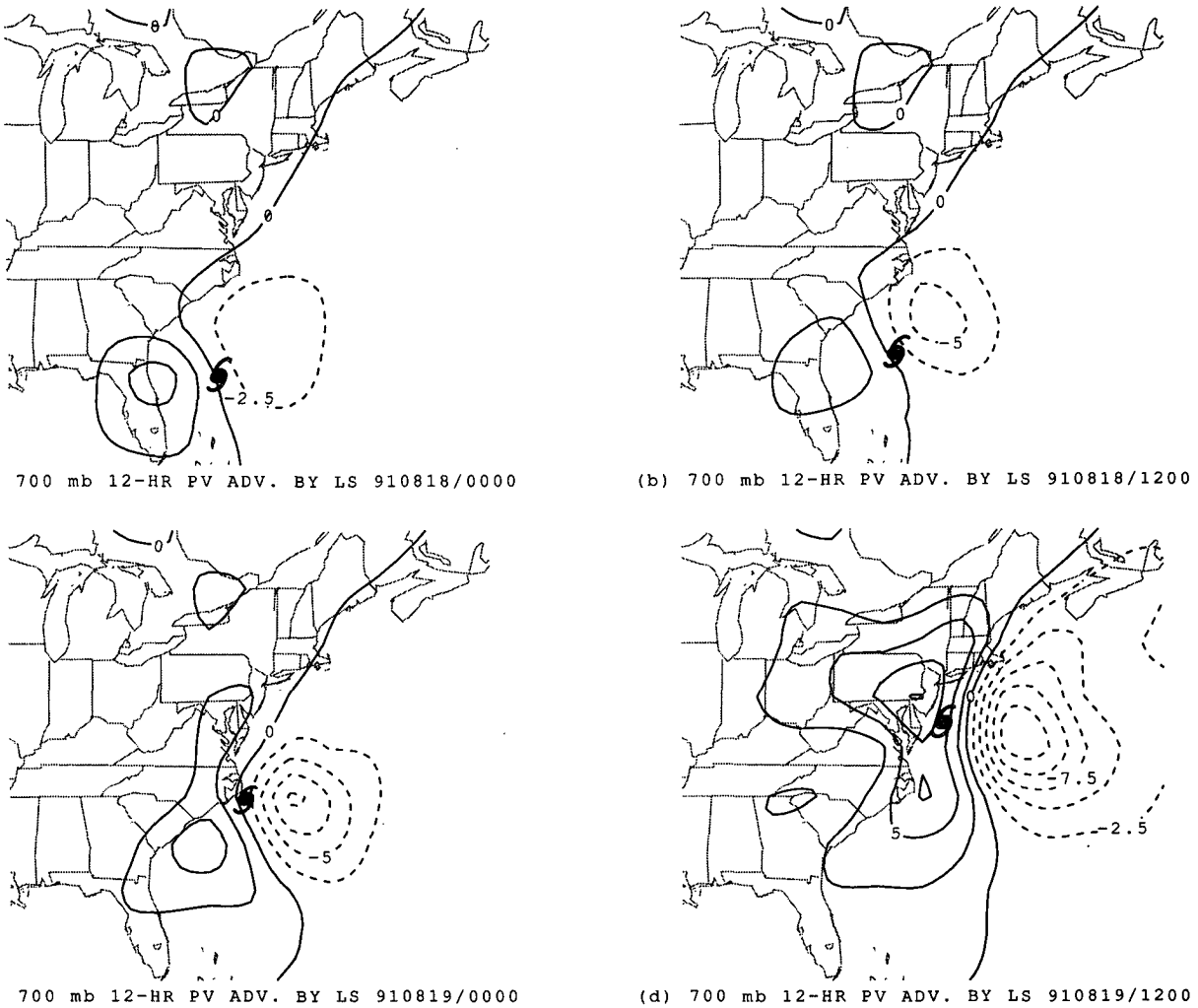

FIG. 14. The 12-h 700-mb Ertel's potential vorticity advection by the balanced flow associated with LS. (a) At 0000 UTC 18, (b) at 1200 UTC 18, (c) at 0000 UTC 19, and (d) at 1200 UTC 19 August 1991. The unit is 0.01 PVU $(12\ h)^{-1}$, and the contour interval is 0.025 PVU $(12\ h)^{-1}$. All positive (negative) values are represented by solid (dashed) lines. Hurricane Bob's best track positions are indicated by the hurricane symbol.

flow (interpolated to the 850–500-mb pressure-averaged balanced vortex center) and hurricane motion for nine different times. These vector differences appear to be random in direction. The statistics from the nine different times show that the average magnitude of the vector errors is 1.8 m s^{-1} with a standard deviation of 0.6 m s^{-1}. The results are similar when using a single-level (700 mb) advection flow (not shown here) or a tropospheric averaged (850–300 mb) advection flow, except that there is a larger vector difference at 0000 UTC 20 August when using the latter. Overall, despite the inherent limitations of the data, the advection flow derived from the PV diagnostics is a fairly good approximation of Bob's real movement. The result indicates that such a PV approach can be useful in understanding hurricane movement. The result also implicitly suggests that, at least for Bob, the primary hurricane circulation has little direct effect (via LS) on its own motion.

As indicated by Fig. 8c, there is a mean westerly vertical shear of about 5 m s^{-1} between 200 and 700 mb over Bob at 1200 UTC 18 August. The advection flow at each level at 0000 and 1200 UTC 19 August is illustrated in the hodographs in Fig. 16. The vertical shear in the advection flow between 200 and 700 mb is a west-southwesterly at 4 m s^{-1} on 0000 UTC 19 August and a southerly at 10 m s^{-1} on 1200 UTC 19 August. In general, Bob's motion correlates most closely with the midtropospheric (850–400 mb) flow, and at these two times, Bob moves north-northwest relative to the defined advection flow.

To deduce how the NMC data would perform in estimating the hurricane steering wind using traditional methods, we use the same data to construct the annular

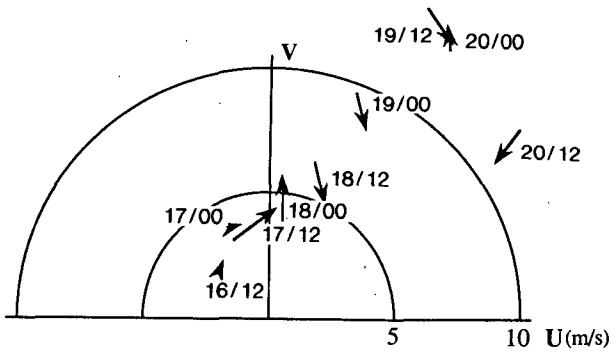

FIG. 15. Velocity vector differences between the 850–500-mb pressure-averaged advection flow and Bob's motion from 1200 UTC 16–20 August 1991. The 850–500-mb pressure-averaged balanced vortex center is used for interpolation.

average wind surrounding the hurricane similar to the 5°–7° band average wind. This is done by averaging the wind field over 28 grids surrounding the hurricane (illustrated in Fig. 17). Figure 18 shows the vector errors between the annular average wind and storm motion. The statistics from the nine different times show that the average magnitude of the vector difference is 2.7 m s^{-1} with a standard deviation of 0.9 m s^{-1}. Although such a steering flow roughly estimates the real storm motion, a quantitative comparison with Fig. 15 shows that vector errors between the traditional method and storm motion are much larger than for the PV approach.

Compared to the annular mean winds, our analysis provides a more dynamically consistent method of determining the advection flow through the hurricane center. In addition, the PV framework is conceptually more concise, and allows one to study the essential dynamical mechanism responsible for hurricane motion.

5. Summary

In this paper, we reviewed the present state of understanding of the concept of hurricane steering (advection), developed a new method to determine the steering (advection) flow of a storm using the PV invertibility principle, and presented a diagnostic study of the motion of Hurricane Bob using potential vorticity methodology. An example of the diagnosis is illustrated for 1200 UTC 18 August. We find that the NMC analyses capture the time evolution of Bob fairly well, except that the gridded analyses typically underestimate Bob's intensity. We also demonstrate that the height and wind fields from the NMC analyses are close to a state of nonlinear balance. We show that the background horizontal PV gradient is concentrated near the tropopause and that the magnitudes of PV anomalies are typically much stronger in the upper troposphere than elsewhere. This is true not only in midlatitudes but also in the subtropics, where some hurricanes originate.

The PV perturbations are separated into three pieces: one including the upper four pressure levels (U) and the other two comprising the lower six levels (LE and LS). Our analysis is able to demonstrate how each individual PV anomaly contributes to Bob's motion. For example, we are able to identify which PV features in U are most influential in advecting Bob. This case study demonstrates that Bob is a hurricane that strongly interacts with midlatitude synoptic-scale upper-level waves.

By studying the time evolution of the PV field, we also investigate the validity of WEM's theoretical hy-

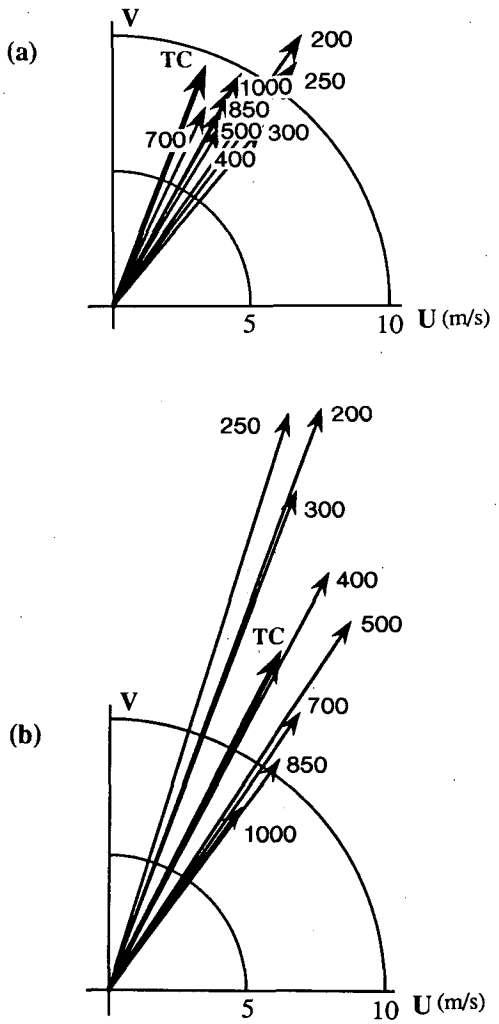

FIG. 16. Velocity vectors of total advection flow at each level and Hurricane Bob's motion at (a) 0000 UTC and (b) 1200 UTC 19 August 1991. The hurricane advection flow is defined as the interpolation of the balanced flows associated with mean, U, and LE to the 850–500-mb pressure-averaged balanced vortex center. TC indicates Bob's motion estimated from every 6-h best track position.

pothesis and the so-called β effect. Our analyses show that an upper-level negative PV anomaly, located above and downshear from Bob, strengthens as Bob evolves. Our preliminary analysis suggests that this negative PV anomaly has a significant effect on Bob's motion, especially at later stages. However, we are not sure how this PV anomaly is generated. Whether this observational analysis supports WEM's hypothesis, that the negative PV anomaly diabatically generated by the hurricane may influence storm motion, is contingent upon our ability of being able to show that the negative PV anomaly aloft (W3 and/or W4) is indeed diabatically produced by Bob itself. More work needs to be done, however, to distinguish which part of the negative PV anomaly (if any) is actually generated by the cyclone.

We also observe that a lower-level negative PV anomaly is always found to the east-northeast of Bob, and this PV anomaly plays an important role in advecting Bob. However, we do not find enough evidence to conclude that this anomaly was developed through the advection by the storm winds of the background PV field.

Finally, we define the hurricane advection flow as the balanced flow, at the storm center, associated with the whole PV distribution, excluding the positive PV anomaly of the hurricane itself. Our results from nine different times indicate that the advection flow derived from our method approximates Bob's actual motion well. We emphasize that an additional advantage of PV diagnostics is that it not only offers a consistent way to detect the flow through the hurricane center but it is also capable of helping to determine how individual dynamical features contribute to the advection of the cyclone.

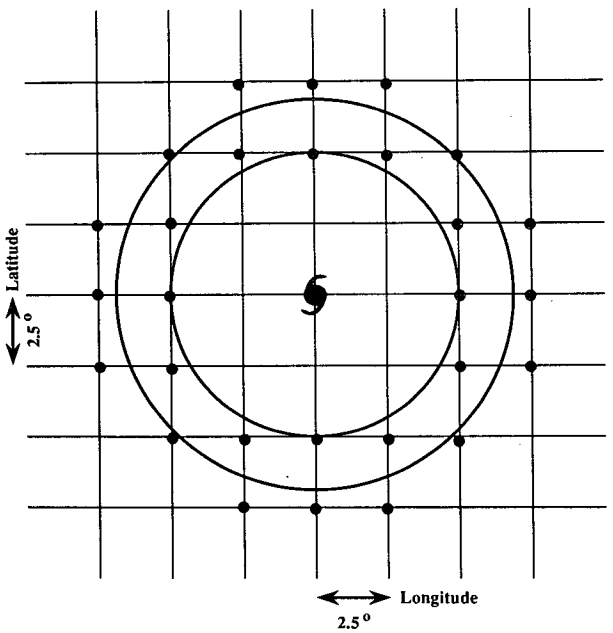

FIG. 17. Illustration of the location of the 28 grids (·) used to mimic the 5°–7° latitude annular average.

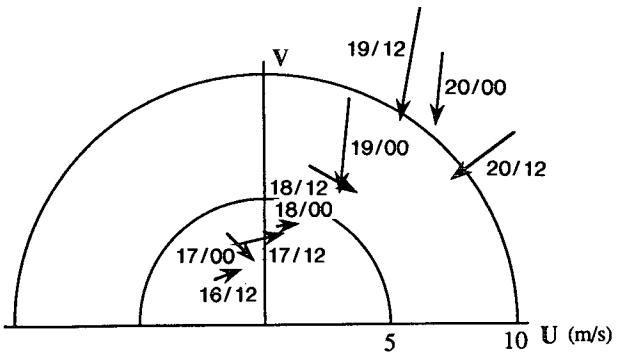

FIG. 18. Velocity vector differences between the 850–500-mb pressure-averaged annular mean flow (interpolated to the 850–500-mb pressure-averaged balanced vortex center) and Bob's motion from 1200 UTC 16–20 August 1991. The 850–500-mb averaged balanced vortex center is used for interpolation.

In a companion paper (Wu and Emanuel 1995), the study of two other cases (Tropical Storm Ana of 1991 and Hurricane Andrew of 1992) will be discussed.

Acknowledgments. This work represents a portion of the first author's Ph.D. dissertation at the Massachusetts Institute of Technology. The authors would like to thank Dr. Christopher Davis for his kind help with the inversion code. The authors also thank Dr. Roger Smith and an anonymous reviewer for their helpful comments. The first author gratefully acknowledges Drs. John Marshall, Glenn Flierl, and Alan Plumb for their valuable suggestions during the course of this work, and Dr. Yoshio Kurihara at GFDL for his support in writing this paper. Credit is also given to Mr. J. Varanyak at GFDL for drafting assistance. This research is supported through the National Science Foundation by Grant ATM-9019615.

REFERENCES

Bengtsson, L. O., 1976: Initial data and some practical aspects of weather forecasting. *NCAR Colloquium on Weather Forecasting and Weather Forecasts: Models, Systems, and Users,* Vol. 1, Boulder, CO, 254–419.

Brand, S., C. A. Buenafe, and H. D. Hamilton, 1981: Comparison of tropical cyclone motion and environmental steering. *Mon. Wea. Rev.,* **109,** 908–909.

Carr, L. E., III, and R. L. Elsberry, 1990: Observational evidence for tropical cyclone propagation relative to environmental steering. *J. Atmos. Sci.,* **47,** 542–546.

Chan, J. C. L., 1985: Identification of the steering flow for tropical cyclone motion from objectively analyzed wind fields. *Mon. Wea. Rev.,* **113,** 106–116.

——, and W. M. Gray, 1982: Tropical cyclone movement and surrounding flow relationship. *Mon. Wea. Rev.,* **110,** 1354–1376.

——, and R. T. Williams, 1987: Analytic and numerical studies of the beta-effect in tropical cyclone motion. Part 1: Zero mean flow. *J. Atmos. Sci.,* **44,** 1257–1264.

Charney, J. G., 1955: The use of primitive equations of motion in numerical prediction. *Tellus,* **7,** 22–26.

Davis, C. A., 1990: Cyclogenesis diagnosed with potential vorticity. Ph.D. dissertation, Massachusetts Institute of Technology, 194 pp.

——, 1992: Piecewise potential vorticity inversion. *J. Atmos. Sci.,* **49,** 1397–1411.

——, and K. A. Emanuel, 1991: Potential vorticity diagnostics of cyclogenesis. *Mon. Wea. Rev.,* **119,** 1925–1953.

Dey, C. H., 1989: The evolution of objective analysis methodology at the National Meteorological Center. *Wea. Forecasting,* **4,** 257–312.

Dong, K., and C. J. Neumann, 1986: The relation between tropical cyclone motion and environmental geostrophic flows. *Mon. Wea. Rev.,* **114,** 115–122.

Fiorino, M., and R. L. Elsberry, 1989: Some aspects of vortex structure related to tropical cyclone motion. *J. Atmos. Sci.,* **46,** 975–990.

Flatau, M., W. H. Schubert, and D. E. Stevens, 1994: The role of baroclinic processes in tropical cyclone motion: The influence of vertical tilt. *J. Atmos. Sci.,* **51,** 2589–2601.

Franklin, J. L., 1990: Dropwindsonde observations of the environmental flow of Hurricane Josephine (1984): Relation to vortex motion. *Mon. Wea. Rev.,* **118,** 2732–2744.

George, J. E., and W. M. Gray, 1976: Tropical cyclone motion and surrounding parameter relationships. *J. Appl. Meteor.,* **15,** 1252–1264.

Haltiner, G. J., and R. T. Williams, 1980: *Numerical Prediction and Dynamic Meteorology.* 2d ed. Wiley and Sons, 477 pp.

Hoskins, B. J., M. E. McIntyre, and A. W. Robertson, 1985: On the use and significance of isentropic potential-vorticity maps. *Quart. J. Roy. Meteor. Soc.,* **111,** 877–946.

Jordan, E. S., 1952: An observational study of the upper wind-circulation around tropical storms. *J. Meteor.,* **9,** 340–346.

Kanamitsu, M., 1989: Description of the NMC global data assimilation and forecast system. *Wea. Forecasting,* **4,** 335–342.

——, J. C. Alpert, K. A. Campana, P. M. Caplan, D. G. Deaven, M. Iredell, B. Katz, H.-L. Pan, J. Sela, and G. H. White, 1991: Recent changes implemented into the global forecast system at NMC. *Wea. Forecasting,* **6,** 425–435.

Kurihara, Y., M. A. Bender, R. E. Tuleya, and R. J. Ross, 1990: Prediction experiments of Hurricane Gloria (1985) using a multiply nested moveable mesh model. *Mon. Wea. Rev.,* **118,** 2185–2198.

Marks, F. D., Jr., R. A. Houze, Jr., and J. F. Gamache, 1992: Dual-aircraft investigation of the inner core of Hurricane Norbert. Part I: Kinematic structure. *J. Atmos. Sci.,* **49,** 919–942.

Miller, B. I., 1958: The use of mean layer winds as a hurricane steering mechanism. U.S. National Hurricane Research Project Rep. No. 18, 24 pp.

——, and P. L. Moore, 1960: A comparison of hurricane steering levels. *Bull. Amer. Meteor. Soc.,* **41,** 59–63.

Molinari, J., 1993: Environmental controls on eye wall cycles and intensity change in Hurricane Allen (1980). *Proc. ICSU/WMO Int. Symp. on Tropical Cyclone Disasters,* Beijing, China, World Meteorological Organization, 328–337.

Montgomery, M. T., and B. F. Farrell, 1993: Tropical cyclone formation. *J. Atmos. Sci.,* **50,** 285–310.

Neumann, C. J., 1979: On the use of deep-layer mean geopotential height fields in statistical prediction of tropical cyclone motion. Preprints, *Sixth Conf. on Probability and Statistics in Atmosphere Sciences,* Banff, Alberta, Canada, Amer. Meteor. Soc., 32–38.

Reeder, M. J., R. K. Smith, and S. J. Lord, 1991: The detection of flow asymmetries in the tropical environment. *Mon. Wea. Rev.,* **119,** 848–855.

——, ——, and ——, 1992: Reply to comments on "The detection of flow asymmetries in the tropical environment." *Mon. Wea. Rev.,* **120,** 2398–2400.

Reilly, D. H., 1992: On the role of upper-tropospheric potential vorticity advection in tropical cyclone formation: Case studies from 1991. Master's thesis, Department of Earth, Atmospheric, and Planetary Sciences, Massachusetts Institute of Technology, 124 pp.

Rotunno, R., and K. A. Emanuel, 1987: An air–sea interaction theory for tropical cyclones: Part II. *J. Atmos. Sci.,* **44,** 542–561.

Roux, F., and F. D. Marks, Jr., 1991: Eyewall evolution in Hurricane Hugo deduced from successive airborne Doppler observations. Preprints, *19th Conf. on Hurricanes and Tropical Meteorology,* Miami, FL, Amer. Meteor. Soc., 558–563.

Shapiro, L. J., 1992: Hurricane vortex motion and evolution in a three-layer model. *J. Atmos. Sci.,* **49,** 140–153.

Smith, R. K., and W. Ulrich, 1993: Vortex motion in relation to the absolute vorticity gradient of the vortex environment. *Quart. J. Roy. Meteor. Soc.,* **119,** 207–215.

——, ——, and G. Dietachmayer, 1990: A numerical study of tropical cyclone motion using a barotropic model. I: The role of vortex asymmetries. *Quart. J. Roy. Meteor. Soc.,* **116,** 337–362.

Trenberth, K. E., and J. G. Olson, 1988: Evaluation of the NMC global analysis: 1979–1987. NCAR Tech. Note TN-259+STR.

Ulrich, W., and R. K. Smith, 1991: A numerical study of tropical cyclone motion using a barotropic model. II: Motion in spatially varying large-scale flows. *Quart. J. Roy. Meteor. Soc.,* **117,** 107–124.

Velden, C. S., and L. M. Leslie, 1991: The basic relationship between tropical cyclone intensity and the depth of the environmental steering layer in the Australian region. *Wea. Forecasting,* **6,** 244–253.

Wu, C.-C., and K. A. Emanuel, 1993: Interaction of a baroclinic vortex with background shear: Application to hurricane movement. *J. Atmos. Sci.,* **50,** 62–76.

——, and ——, 1994: On hurricane outflow structure. *J. Atmos. Sci.,* **51,** 1995–2003.

——, and ——, 1995: Potential vorticity diagnostics of hurricane movement. Part II: Tropical Storm Ana (1991) and Hurricane Andrew (1992). *Mon. Wea. Rev.,* **123,** 93–109.